Glycinergic tonic inhibition of hippocampal neurons with depolarizing GABAergic transmission elicits histopathological signs of temporal lobe epilepsy

Sabrina A. Eichler [a], Sergei Kirischuk [b], René Jüttner [c], Philipp K. Schafermeier [a], Pascal Legendre [d], Thomas-Nicolas Lehmann [e], Tengis Gloveli [f], Rosemarie Grantyn [b], Jochen C. Meier [a], *

[a] *RNA Editing and Hyperexcitability Disorders Helmholtz Group, Max Delbrück Center for Molecular Medicine, Berlin, Germany*
[b] *Developmental Physiology, Institute for Neurophysiology, Charité University Medicine Berlin, Germany*
[c] *Developmental Neurobiology, Max Delbrück Center for Molecular Medicine, Berlin, Germany*
[d] *UMR CNRS 7102 NPA, Université Pierre et Marie Curie, Paris, France*
[e] *Department of Neurosurgery, Charité University Medicine Berlin, Germany*
[f] *Cellular and Network Physiology, Institute of Neurophysiology, Charité University Medicine Berlin, Germany*

Abstract

An increasing number of epilepsy patients are afflicted with drug-resistant temporal lobe epilepsy (TLE) and require alternative therapeutic approaches. High-affinity glycine receptors (haGlyRs) are functionally adapted to tonic inhibition due to their response to hippocampal ambient glycine, and their synthesis is activity-dependent. Therefore, in our study, we scanned TLE hippocampectomies for expression of haGlyRs and characterized the effects mediated by these receptors using primary hippocampal neurons. Increased haGlyR expression occurred in TLE hippocampi obtained from patients with a severe course of disease. Furthermore, in TLE patients, haGlyR and potassium chloride cotransporter 2 (KCC2) expressions were inversely regulated. To examine this potential causal relationship with respect to TLE histopathology, we established a hippocampal cell culture system utilising tonic inhibition mediated by haGlyRs in response to hippocampal ambient glycine and in the context of a high Cl^- equilibrium potential, as is the case in TLE hippocampal neurons. We showed that hypoactive neurons increase their ratio between glutamatergic and GABAergic synapses, reduce their dendrite length and finally undergo excitotoxicity. Pharmacological dissection of the underlying processes revealed ionotropic glutamate and TrkB receptors as critical mediators between neuronal hypoactivity and the emergence of these TLE-characteristic histopathological signs. Moreover, our results indicate a beneficial role for KCC2, because decreasing the Cl^- equilibrium potential by KCC2 expression also rescued hypoactive hippocampal neurons. Thus, our data support a causal relationship between increased haGlyR expression and the emergence of histopathological TLE-characteristic signs, and they establish a pathophysiological role for neuronal hypoactivity in the context of a high Cl^- equilibrium potential.

Keywords: hippocampus ● epilepsy ● glycine receptor ● RNA editing ● inhibition ● E-I balance ● tonic inhibition ● KCC2 ● excitotoxicity ● synapse elimination

Introduction

Information transfer in the brain requires a homeostatic control of neuron excitability. A deregulation of the homeostatically balanced ratio between glutamatergic and GABAergic synapses (Glu/GABA ratio) is considered to elicit hyperexcitability, as is the case with temporal lobe epilepsy (TLE) [1, 2]. Therefore in TLE, plasticity of GABAergic inhibitory signalling attracted much attention, and previous research identified several anticonvulsive substances that enhance tonic GABAergic inhibition to compensate for increased Glu/GABA ratios of synaptic input (for review see [3]).

Glycine receptors (GlyRs) are homologous to GABA$_A$ receptors (GABA$_A$Rs), and transgenic mice expressing β-galactosidase instead of GlyR α$_3$ (strain: B6.129P2-*Glra3*^{tm1Dgen}/J, stock: 005816, The Jackson Laboratory, JAX® Mice and Services, ME, USA) were found to require lower doses of the GABA$_A$R antagonist metrazol to develop various types of epilepsies, suggesting an anticonvulsive potential of GlyRs. Indeed, recent evidence has

*Correspondence to: Dr. Jochen C. MEIER,
Max Delbrück Center for Molecular Medicine,
Robert-Rössle-Strasse 10,
13092 Berlin, Germany.
Tel.: +49-(0)30-94063062
Fax: +49-(0)30-94063819
E-mail: jochen.meier@mdc-berlin.de

accentuated their contribution to tonic hippocampal inhibition in response to hippocampal ambient glycine [4–10], and glycine and taurine as well as glycine uptake inhibitors were found to be anticonvulsive [7, 11, 12].

However, classical GlyRs have a rather low affinity for glycine [13, 14], while the hippocampal ambient glycine concentration is in the submicromolar range [15, 16]. A *priori*, this discrepancy argues against a role for GlyRs in hippocampal tonic inhibition, but a clarifying possibility is that activity-dependent up-regulation of RNA-edited high-affinity GlyRs (haGlyRs) [17] occurs and thereby approximates the responsiveness of hippocampal GlyRs to the level of hippocampal ambient glycine.

To investigate this possibility, we scanned human TLE hippocampi for haGlyR expression. Up-regulation of α_2- and α_3-haGlyR expression indeed occurred in TLE hippocampi obtained from patients with a severe course of disease. Furthermore, an *in vitro* cell culture system was developed for characterization of the potential consequences of haGlyR-mediated tonic inhibition. Because down-regulation of the potassium chloride cotransporter 2 (KCC2) is a hallmark of TLE hippocampi [18–20], primary rat hippocampal neurons were investigated at a time-point when the Cl^- equilibrium potential was still high. Tonic activation of haGlyRs rendered these hippocampal neurons hypoactive and elicited histopathological characteristics of TLE hippocampi, in terms of elevated Glu/GABA ratios of synaptic input, abnormal dendrite length growth and a pronounced susceptibility of neurons to excitotoxic degeneration. Decreasing the Cl^- equilibrium potential by KCC2 expression restored hippocampal neurons. On the basis of these results we propose that up-regulation of haGlyRs enhances tonic inhibition of hippocampal neurons and contributes to the pathogenesis of TLE, provided that the neuronal Cl^- equilibrium potential is high.

Materials and methods

Detection of haGlyRs in hippocampi from TLE patients

Analysis of resected human hippocampi was performed according to the rules laid down by the Ethics Commission (Charité, EA1/142/05), and informed consent was received from all patients. The relative amounts of haGlyRs α_2^{192L} and α_3^{185L} were determined in hippocampal specimen of patients suffering from pharmacoresistant TLE. The degree of hippocampal cell loss was categorized according to the Wyler classification [21]. Tissue samples from TLE patients obtained by removal of the rostral part of the hippocampus were stored in liquid nitrogen immediately after resection. Total RNA was then isolated using TRIzol Reagent (Invitrogen Life Technologies, Carlsbad, CA, USA). cDNA was obtained by reverse transcription (Superscript II, Invitrogen) of 2 μg RNA with equimolar mixtures of 3′-anchored poly-T oligonucleotides ($T_{18}V$, $T_{15}V$, $T_{13}V$). The haGlyR detection assay was performed as previously described [17], except that *Bsp*EI was used instead of *Hind*III. Due to mispriming of the oligonucleotides,

polymerase chain reaction (PCR) amplification was set up as a touch-up protocol (annealing: $5 \times 52°C$, $30 \times 56°C$ for GlyR α_2, and $5 \times 54°C$, $35 \times 58°C$ for GlyR α_3). Regions spanning exon 5 were amplified using oligonucleotides 5′-GGAAGGATCCCACGGCTGGCG-3′ and 5′-GTTC-CTTCTCTTCTTTCAAAATAATCCGG-3′ (GlyR α_2), and 5′-GAGACGACCATG-GATCCCAGAGTG-3′ and 5′-CGTAAATCTTTTTCTTCTTTCAACAGTATCCGG-3′ (GlyR α_3). Note that in cases of 554T and 575T, the 3′-ends of the respective oligonucleotides (TCCGG) are elongated according to a full *Bsp*EI site. The respective sense oligonucleotides introduced *Bam*HI restriction sites. For subsequent cloning *Bam*HI and *Bsp*EI (New England Biolabs, Hertfordshire, UK) were used. Positive (α_2^{575T} and α_3^{554T}) and negative (α_2^{575C} and α_3^{554C}) control clones were always processed simultaneously. Amplified control clones were digested with 10 units each of *Bam*HI and *Bsp*EI for 2 hrs at 37°C, and for amplified cDNA of TLE patients the amount of restriction enzymes was adjusted proportionally to rule out any relaxed enzyme activity. Equimolar amounts of double-digested cloning vector (modified pBluescript SK II vector, into which a *Bsp*EI site was introduced) and of samples were ligated using the Rapid DNA Ligation Kit (Fermentas GmbH, St. Leon-Rot, Germany). Following transformation of JM109 competent bacteria (Promega, Madison, WI, USA), the number of true positive colony forming units (cfu) was determined by PCR on cfu. The respective oligonucleotides for PCR on cfu were T7 (5′-GTAATACGACTCAC-TATAGGGC-3′) in combination with 5′-ACCCATCCATGCTAGACTCC-3′ (GlyR α_2) or 5′-TCAAGAATTTTCCCATGGATGTA-3′ (GlyR α_3). The amount of haGlyRs in human hippocampi was expressed as a percentage fraction of the number of true positive cfu obtained from human samples and the number of true positive cfu obtained from the respective positive control clone. At least three experiments per human hippocampus were performed. For surveillance of the detection procedure a calibration curve (Supplementary Fig. 1B) was obtained by amplifying control clone DNA mixtures containing increasing amounts (%: 1, 2.5, 5, 10, 25, 50, 75) of positive control clones. Again, 0% and 100% of positive control clones served as negative and positive control reactions, respectively.

Detection of human GlyR α_2A and α_2B transcripts in hippocampi from TLE patients

The relative mRNA levels encoding alternatively spliced human GlyR $\alpha2A$ and $\alpha2B$ subunits were determined by PCR using $\alpha2A$- and $\alpha2B$-specific oligonucleotides 5′-ATCAACAGTTTTGGATCAGTCA-3′ ($\alpha2A$) and 5′-TCAACAGCTTTGGGTCAATAG-3′ ($\alpha2B$), respectively, in combination with 5′-CCTTCAGCAACTTGCACTGG-3′, which binds downstream of the alternatively spliced exon 3. Annealing was set to 58°C, 30 cycles were run. GlyR $\alpha2A$- and $\alpha2B$-specific PCRs had to be performed in separate reactions because $\alpha2A$- and $\alpha2B$-specific PCR products were of the same size. Agarose gel-separated PCR products were quantified using ImageQuant software (Molecular Dynamics, Sunnyvale, CA, USA) and expressed as mean pixel intensity. Triplicate experiments were performed, and the ratio between intensities of $\alpha2A$ and $\alpha2B$ products was extracted from each experiment. Average ratios below a value of 0.5 were designated 'B', between 0.5 and 1.5 were designated 'AB' and above 1.5 were denominated 'A' (Fig. 1D).

Semiquantitative analysis of KCC2 expression in hippocampi from TLE patients

KCC2 and β-actin were always co-amplified in the same PCR reaction tubes using oligonucleotides (10 μM each, 5′-CTGCTGGCTTACCTCTTCC-3′
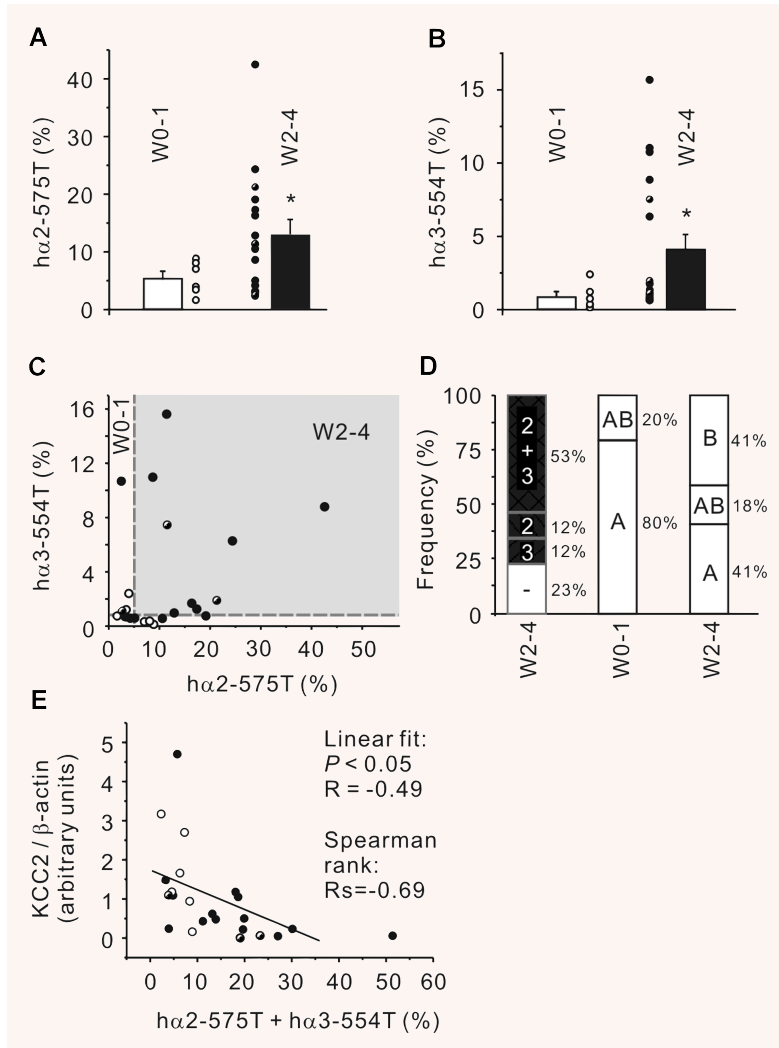
Fig. 1 Hippocampal damage and reduction of KCC2 expression are associated with elevated human haGlyR expression in TLE hippocampi. (**A**, **B**) Relative amounts of haGlyRs $\alpha2^{575T}$ and $\alpha3^{554T}$ detected in hippocampi from epilepsy patients without (W0–1, cell loss <10%) and with (W2–4, cell loss > 10%) hippocampal cell loss (see Table 1 for anamnesis of TLE patients). The latter includes patients with frequent SGTCS ($\geq$1/month), but without hippocampal damage (three patients). Individual patient scores are shown as open (W0–1, n = 6), filled (W2–4, n = 17) and dashed (SGTCS $\geq$ 1/month, n = 3) circles. Columns illustrate means $\pm$ S.E.M. (**C**) GlyR $\alpha2^{575T}$ fractions plotted against $\alpha3^{554T}$ fractions. Dashed lines indicate W0–1 mean $\alpha2^{575T}$ and $\alpha3^{554T}$ fractions, respectively. (**D**) Percentages of patients with suprathreshold (> mean of W0–1) $\alpha2^{575T}$ + $\alpha3^{554T}$ (2 + 3), $\alpha2^{575T}$ (2) and $\alpha3^{554T}$ (3) fractions, respectively. Ratios between GlyR $\alpha2A$ and $\alpha2B$ mRNAs were determined. Average ratios below a value of 0.5 were designated 'B', between 0.5 and 1.5 were designated 'AB' and above 1.5 were denominated 'A'. Note that prevailing expression of GlyR $\alpha2B$ transcripts ('B') is associated with hippocampal damage and a high SGTCS frequency in W2–4 patients. (**E**) Inverse correlation between KCC2 (normalized to β-actin) and haGlyR expression levels in hippocampi from TLE patients. Error bars indicate the S.E.M. of the mean values obtained from at least three independent experiments. Significance level is $P < 0.05$ (*).

and 5′-CGTCTCATTTCCTTCCCAAG-3′, KCC2) and (5 μM each, 5′-CGCTCGTTGCCAATAGTGATG-3′ and 5′-TTGTAACAAACTGGGACGAT ATGG-3′, β-actin). Annealing was set to 58°C; 30 cycles were run. PCR products were separated by agarose gel electrophoresis, quantified using ImageQuant software (Molecular Dynamics) and expressed as mean pixel intensity. The relative KCC2 expression level was expressed as the mean pixel intensity of KCC2 divided by the mean pixel intensity of β-actin.

Hippocampal cell culture and transfection

All animals were killed according to the permit (LaGeSo, 0122/07) given by the Office for Health Protection and Technical Safety of the regional government of Berlin and in compliance with regulations laid down in the European Community Council Directive. Hippocampal cultures from E19 *Wistar* rats were prepared as previously described [6] and maintained in B27- and 1% FCS-supplemented Neurobasal medium [22]. The initial cell density was 68,000/cm^2. Transfection was carried out on day(s) *in vitro* (d.i.v.) 6, as described [17], using plasmids encoding the short (K) splice

variants of GlyR $\alpha3$ [14]. GlyRs $\alpha3K^{185P}$ or $\alpha3K^{185L}$ will henceforth be referred to as $\alpha3^{185P}$ or $\alpha3^{185L}$. In part of the experiments, KCC2 (generous gifts from Claudio Rivera and Karl Kandler) was cotransfected with GlyRs. The KCC2 expression construct provided by Karl Kandler uses a pMES vector backbone, which was originally produced by Catherine Krull [23]. This allowed the use of enhanced green fluorescent protein (EGFP) as an indicator for KCC2 expression [24]. Caspase-3 sensor was used as an indicator for apoptosis [25]. For transfection, coverslips were transferred to wells containing transfection medium (Neurobasal supplemented with 0.25 mM glutamine) and were incubated with complexes formed with 5 μl of effectene transfection reagent (Qiagen, Hilden, Germany) and 300 ng of DNA. The Qiagen transfection protocol was followed, except that the incubation time was reduced to 1 hr. This protocol ensured moderate expression levels of the transfected proteins within 3 days in ~1% of hippocampal neurons. The coverslips were then transferred into new dishes containing a culture medium with low glycine content. Glycine- and serum-free minimal essential medium was supplemented with D-glucose (25 mM), HEPES (10–20 mM), Na-pyruvate (230 μM), vitamin B$_{12}$ (0.2 μM), L-glutamine (250 μM), β-mercaptoethanol (25 μM),

B27-supplement and 5 μM glycine, which corresponds to the EC_{50} of GlyR $\alpha 3^{185L}$. The concentration of 5 μM glycine was maintained throughout all experiments, also during electrophysiological recordings.

Whole-cell and perforated patch clamp recording of hippocampal neurons in culture

Whole-cell and perforated patch clamp recordings were made from neurons expressing $\alpha 3^{185P}$ or $\alpha 3^{185L}$ GlyRs together with the EGFP, which allowed selection of transfected cells by fluorescence microscopy. Access resistance was monitored throughout the experiments. Serial resistance compensation was not applied. Measurements were not corrected for liquid junction potentials. Electrophysiological signals were acquired using an EPC-7 amplifier (List, Darmstadt, Germany), a 16-bit AD/DA board (ITC-16, HEKA Elektronik, Lambrecht, Germany), and TIDA 4.11 software (HEKA Elektronik). The signals were filtered at 3 kHz and sampled at a rate of 10 kHz.

Whole-cell recordings were performed in the standard salt solution (SSS). The intrapipette solution contained (in mM): potassium gluconate (100), KCl (50), NaCl (5), $CaCl_2$ (0.5), EGTA (5) and HEPES (25); pH was set to 7.2 with KOH. Pipette resistance was 3–5 MΩ when filled with the above saline. Access resistance was monitored by applying hyperpolarizing pulses of 10 mV. Cell capacitance (C_m) and access resistance values were obtained by fitting a monoexponential function to the capacitance artefacts. Only recordings with a series resistance below 40 MΩ were accepted. Cells exhibiting more than 20% changes in the access resistance during an experiment were discarded. Miniature postsynaptic currents (PSCs) were recorded in the presence of 1 μM tetrodotoxine at the holding potential of -70 mV. Action potentials (APs) were recorded in the current clamp mode. Current injection was used to hold cells at about -70 mV. Firing patterns were elicited by 500 ms, suprathreshold depolarizing pulses. AP threshold was determined as the point where the first derivative started to increase. AP duration was measured at the level of AP threshold.

Perforated patch clamp experiments were performed in the SSS supplemented with 1 μM tetrodotoxin to block AP generation. SSS containing glycine (100 μM) was applied locally *via* a glass pipette positioned in the vicinity (about 100 μm) of a cell of interest. Recording electrodes (3–5 MΩ) were filled with gramicidin (25–50 μg/ml) and Fura-2-K_5 (0.3 mM) in a solution containing (in mM): potassium gluconate (100), KCl (50), NaCl (5), $CaCl_2$ (0.5), EGTA (5) and HEPES (25); pH was set to 7.2 with KOH. Fura fluorescence was monitored at an excitation wavelength of 360 nm to confirm that the perforated patch configuration was maintained. The access resistance was monitored throughout experiments. After 30–40 min it stabilized at 40–50 MΩ. Cells exhibiting more than 20% changes in the access resistance during an experiment were discarded.

Ca^{2+} Imaging of hippocampal neurons in culture

For Ca^{2+} imaging, cultures were placed into a recording chamber (~0.4 ml volume) on the microscope stage (Axioscope FS, Zeiss, Oberkochen, Germany) equipped with phase contrast optics. Cultures were submerged with a constant flow of SSS (pH 7.4) containing (in mM): NaCl (140), KCl (3), $MgCl_2$ (1), $CaCl_2$ (2), HEPES-NaOH (20) and glucose (30). Flow rate was set to 0.5 ml/min using a gravity-driven, manually operated superfusion system. A 40$\times$ water immersion objective (Zeiss) was used in all experiments. Experiments were performed at room temperature (23–25°C). Measurements of cytoplasmic Ca^{2+} transients were performed using a Ca^{2+}-sensitive fluorescent dye, Fura-2 (Molecular Probes, Eugene, OR, USA). Cells were loaded through incubation in the SSS supplemented with Fura-2 acetomethylester (Fura-2/AM, 5 μM) and Pluronic F-127 (0.02%) for 20 min at 36°C. Subsequently, cultures were incubated for 30 min in the SSS at room temperature to ensure Fura-2/AM deesterification. Excitation wavelength was controlled by a fast monochromator system, and fluorescence signals were recorded by a CCD camera (TILL Photonics, Munich, Germany). For cell selection, EGFP was excited using 490 nm light. Fura-2 was excited alternatively at 360 and 380 nm. Excitation and emission light were separated by a 510-nm dichroic mirror. The emitted light was filtered using a 530-nm longpass filter. All measurements were performed at 4 $\times$ 4 binning. Exposure time was set to 200 ms. Acquisition rate for $[Ca^{2+}]$ measurement was set to one pair of images per 1 sec. The background fluorescence was calculated from a region in the immediate vicinity of the cell of interest and subtracted. Fluorescence signals were expressed as the ratio of fluorescence recorded at 360 and 380 nm excitation wavelengths (F_{360}/F_{380}).

Antibodies

GlyRs were recognized by the monoclonal antibody mAb4a [26] (1:200, Synaptic Systems GmbH, Göttingen, Germany). The vesicular GABA transporter (VGAT) and vesicular glutamate transporters (VGluT) were visualized with polyclonal antibodies from rabbit [27] (1:200, Synaptic Systems GmbH) and guinea pig [28] (1:500, Chemicon, Temecula, CA, USA), respectively. Endogenous KCC2 was visualized with a rabbit polyclonal antibody [29] (Upstate, Charlottesville, VA, USA). EGFP indicated the presence of KCC2 [23] in GlyR/KCC2 co-expression experiments. After methanol/glacial acetic acid fixation, which cuts off YFP fluorescence, EYFP protein as part of the caspase-3 sensor was detected with a polyclonal anti-GFP antibody (Invitrogen Life Technologies) and a secondary fluorescein isothiocyanate (FITC)-coupled antibody. For multiple labelling experiments, monoclonal and polyclonal antibodies were combined. Secondary antibodies were coupled to carboxymethyl-indocyanine (Cy3, Cy5), FITC or Alexa350 and purchased from Jackson ImmunoResearch Laboratories (West Grove, PA, USA) or Molecular Probes, respectively. Coverslips were mounted in Vectashield medium (Vector Laboratories, Burlingame, CA, USA).

Immunofluorescence

Cells were immersed into a mixture (95/5) of methanol and glacial acetic acid for 10 min at -20°C. Appropriate filters (XF22, XF32, XF110-2, XF136-2; Omega Optical Inc., Brattleboro, VT, USA) allowed the detection and separation of fluorescence signals. To ensure that labelling was specifically due to the primary antibodies, we replaced the latter with similarly diluted normal serum from the same species. Our methods for evaluation of presynaptic terminal number and dendrite morphology in dissociated hippocampal cultures were previously described [30, 31]. Briefly, labelled neurons were visualized by standard epifluorescence under a plan-neoflur 40$\times$ oil objective with a numerical aperture of 1.3 (Zeiss). Images were acquired using a 14-bit cooled CCD camera (Spot PURSUIT, Visitron Systems GmbH, Puchheim, Germany) and software Metamorph (Universal Imaging Corp., Downingtown, PA, USA). Terminal counts and analysis of dendrite morphology were performed manually. A circular region of interest (ROI) with a diameter of 100 μm was projected onto GlyR-expressing neurons, its centre roughly coinciding with the centre of the soma. Suitable viewfields were photographed from triple-stained

(VGluT, VGAT, GlyR) preparations, and Glu/GABA ratios were extracted from each transfected neuron. To avoid false positives in synaptic terminal counts, we applied a size criterion. Assuming a round shape of the contact, a synaptic terminal was requested to have a suprathreshold intensity over an area with a diameter between 0.5 and 2 μm, the threshold intensity being equal to the average intensity of the ROI plus three times its standard deviation. Dendritic length was characterized as the number of dendrites that exceeded the limit of the ROI (abbreviated as 'dendrites > 50 μm'). The fraction of apoptotic and degenerated neurons, which expressed $\alpha3^{185P}$ or $\alpha3^{185L}$ was evaluated using caspase-3 sensor co-expression and morphological criteria, the latter according to the presence of dendritic swellings and varicosities [32].

Statistics

Numerical data are reported as mean $\pm$ standard error of means (S.E.M.). In hippocampal cell culture experiments, neurons were sampled from at least three different cultures, each including at least 20 viewfields from two different coverslips. Molecular biology experiments conducted on TLE patients were performed in triplicate. If not stated otherwise, statistical analysis (unpaired Student's t-test, ANOVA and Mann-Whitney) was performed using the software Origin (Microcal, Northampton, MA, USA). Significance levels are indicated in the figures as *$P <$ 0.05, **$P <$ 0.01, ***$P <$ 0.001.

Reagents

In part of the experiments the medium was supplemented with iGluR antagonists DNQX (6,7-dinitroquinoxaline-2,3(1H,4H)-dione, 20 μM) and/or MK801 (dizocilpine, 1 μM, both from Tocris, Bristol, UK) and/or the tyrosine kinase inhibitor K252a (200 nM, Sigma-Aldrich, Deisenhofen, Germany). The culture medium was supplemented with these drugs during GlyR expression, *i.e.* from d.i.v. 6 to d.i.v. 9.

Results

Elevated haGlyR expression occurs in hippocampi from TLE patients with a severe course of disease

Human TLE hippocampi resected for therapeutic reasons were screened for elevated expression of haGlyRs. According to the severity of their course of disease, TLE patients were divided in two groups (Table 1, 'internal grading'). Patients without remarkable hippocampal cell loss (Wyler 0–1, cell loss <10%) and a low frequency (<1/month) of secondarily generalized bilateral tonic–clonic seizures (SGTCS) were designated W0–1 (Table 1). Patients with remarkable hippocampal cell loss (Wyler 2–4, cell loss > 10%) or a high SGTCS frequency (≥1/month) were termed W2–4 (Table 1). The experimental strategy [17] for detection of haGlyRs was adapted to human cDNA sequences and validated by calibration (Supplementary Fig. 1A and B).

In human TLE hippocampi haGlyR $\alpha2^{192L}$ (575T, Supplementary Fig. 1A) and $\alpha3^{185L}$ (554T) were detected (Fig. 1A and B). Compared with W0–1 TLE patients $\alpha2^{575T}$ and $\alpha3^{554T}$ haGlyR mRNA fractions of $\alpha2$ and $\alpha3$ transcripts were elevated in W2–4 patients (W0–1 [%]: $\alpha2^{575T}$: 5.5 $\pm$ 1.2; $\alpha3^{554T}$: 0.9 $\pm$ 0.3, $n = 6$ patients; W2–4 [%]: $\alpha2^{575T}$: 12.8 $\pm$ 2.5; $\alpha3^{554T}$: 4.1 $\pm$ 1.2, $n = 17$, thereof 14 Wyler 2–4 patients and 3 Wyler 0–1 patients with a high SGTCS frequency). Seven Wyler 2–4 patients and two Wyler 0–1 patients with frequent SGTCS were characterized by congruent incidences of haGlyRs $\alpha2^{575T}$ and $\alpha3^{554T}$, exceeding the respective W0–1 mean values (Fig. 1C and D; 9/17 ~ 53%). Twelve per cent (2/17) of Wyler 2–4 patients expressed increased levels of haGlyR $\alpha2^{575T}$ only, and suprathreshold expression of haGlyR $\alpha3^{554T}$ only was found in one Wyler 2–4 patient and one Wyler 0–1 patient with frequent SGTCS (2/17 ~ 12%). Twenty-three per cent (4/17) of W2–4 patients did not differ from W0–1 patients with respect to $\alpha2^{575T}$ and $\alpha3^{554T}$ mRNA levels. In total, compared with W0–1 patients, 77% (13/17) of W2–4 patients were characterized by increased expression of at least one type of haGlyRs. The fact that increased expression of both GlyR $\alpha2^{575T}$ and $\alpha3^{554T}$ was detected in two out of three Wyler 0–1 cases with frequent SGTCS emphasizes the activity dependency of haGlyR expression [17] and accentuates their potential involvement in TLE.

Elevated haGlyR expression accompanies elevated GlyR $\alpha2B$ expression and inversely correlates with KCC2 expression in hippocampi from TLE patients

GlyR $\alpha2$ mRNA is alternatively spliced by insertion of either exon3A or exon3B, and GlyR $\alpha2B$ was shown to be more sensitive to glycine than GlyR $\alpha2A$ [13]. This differential agonist sensitivity is conserved in the case of P192L amino acid substitution, which renders GlyR $\alpha2B^{192L}$ a highly sensitive receptor variant (Supplementary Fig. 1D; EC$_{50Gly}$ [μM]: $\alpha2A^{192L}$: 10.6; $\alpha2B^{192L}$: 3.4). Notably, still ~15% of the maximal current amplitude produced by $\alpha2B^{192L}$ was obtained with submicromolar (0.1 μM) glycine. We therefore quantified the amount of alternatively spliced *Glra2* transcripts in TLE hippocampi. Prevailing expression of GlyR $\alpha2B$ transcripts was found in W2–4 patients (Fig. 1D; 41%, 7/17). Among these cases, 5/17 W2–4 patients expressed W0–1 suprathreshold amounts of both GlyR $\alpha2^{575T}$ and $\alpha3^{554T}$ (thereof two Wyler 0–1 patients with frequent SGTCS). One Wyler 2–4 patient with prevailing GlyR $\alpha2B$ expression was characterized by elevated expression of GlyR $\alpha3^{554T}$ only, and another Wyler 2–4 patient did not show elevated haGlyR expression. Thus, prevailing GlyR $\alpha2B$ expression accompanies elevated expression of haGlyRs $\alpha2^{575T}$ and $\alpha3^{554T}$ in W2–4 patients.

Several studies have accentuated KCC2 down-regulation as a critical step towards the pathophysiology of TLE [18–20, 33, 34]. We therefore analyzed KCC2 expression in hippocampi from W0–1 and W2–4 patients, related it to haGlyR mRNA fractions of GlyR $\alpha2$ and $\alpha3$ transcripts and found an inverse correlation between KCC2 and haGlyR expression (Fig. 1E).

Table 1 Anamnesis of TLE patients

Patient no.	Gender	Age	Seizure types	Seizure frequency	Seizures since (y)	Hippo-campus	Wyler grade	Previous medication	Medication at operation	Internal grading
2.1.3	F	29	CPS SGTCS	1-4/m 1/y	26	Left	0	CBZ	OXC, Frisium	W0-1
2.22.5	F	32	CPS	1/m	4	Right	0 (DNT WHO grade I)	CBZ	LEV	W0-1
2.26.4	M	43	CPS	3-5/m	12	Left	0 (FCD)	CBZ	LEV, GBT	W0-1
2.34.4	F	47	CPS	2-3/m	32	Left	1	CBZ, LTG, PHT, OXC, TPX, VPA, LEV	LTG, Frisium	W0-1
2.50.3	M	38	CPS	4/m	1	Left	0	CBZ, OXC	OXC	W0-1
6.25.5	F	24	CPS	4-6/m	7	Left	0 (FCD)	CBZ	TPX, OXC	W0-1
2.49.4	F	45	SGTCS	2-3/m	22	Left	0	CBZ, LTG, PHT, OXC, TPX, VPA, LEV	GBT	W2-4
6.25.6	F	37	CPS SGTCS	2-3/m 2/m	10	Right	0-1	CBZ	LEV, TPX	W2-4
6.25.7	F	51	CPS SGTCS	2-7/m 1-2/m	11	Right	1	CBZ	LTG	W2-4
2.47.5	F	39	CPS	4-10/m	39	Left	2	CBZ, LTG, PHT, OXC, TPX, VPA, LEV	LTG, LEV	W2-4
2.58.9	F	48	CPS	12-16/m	20	Left	2	CBZ	LTG	W2-4
2.115.7	F	48	CPS	2/m	45	Right	2	CBZ	CBZ	W2-4
2.58.3	F	24	CPS SGTCS	4/m 1/m	7	Right	2-3	CBZ, LTG	LTG	W2-4
2.74.3	M	34	CPS	4-5/m	17	Right	2-3	CBZ, OXC	LEV	W2-4
2.84.4	M	42	CPS	30/m	38	Left	2-3	CBZ	LEV, LTG	W2-4
2.88.4	F	34	SPS	8/m	31	Right	3 (SWD)	CBZ	LTG	W2-4
6.50.3	F	48	SPS SGTCS	2/m 1/m	18	Right	3	CBZ	CBZ, LTG	W2-4
6.50.4	M	15	CPS	1-3/m	6	Left	3	CBZ	CBZ, LTG	W2-4
2.25.5	F	53	CPS	4/m	38	Left	4	CBZ	OXC	W2-4
2.58.11	M	36	CPS	4-5/m	6	Left	4	CBZ	LTG	W2-4
2.92.4	F	49	SPS	3-6/m	22	Left	4	CBZ	LTG	W2-4
2.115.5	F	48	CPS	4-12/m	44	Left	4	CBZ	LTG	W2-4
6.25.8	M	58	CPS	4/m	23	Right	4	CBZ, VPA	OXC, LEV	W2-4

Abbreviations: m: month(s); y: year(s); SPS: simple partial seizures, CPS: complex partial seizures, SGTCS: secondarily generalized bilateral tonic–clonic seizures, OXC: oxcarbazepine, LEV: levetiracetam, GBT: gabapentin, CBZ: carbamazepine, LTG: lamotrigine, PHT: phenytoin, TPX: topiramate, VPA: valproic acid, SWD: Sturge–Weber disease, FCD: focal cortical dysplasia and DNT: dysembryoplastic neuroepithelial tumour.
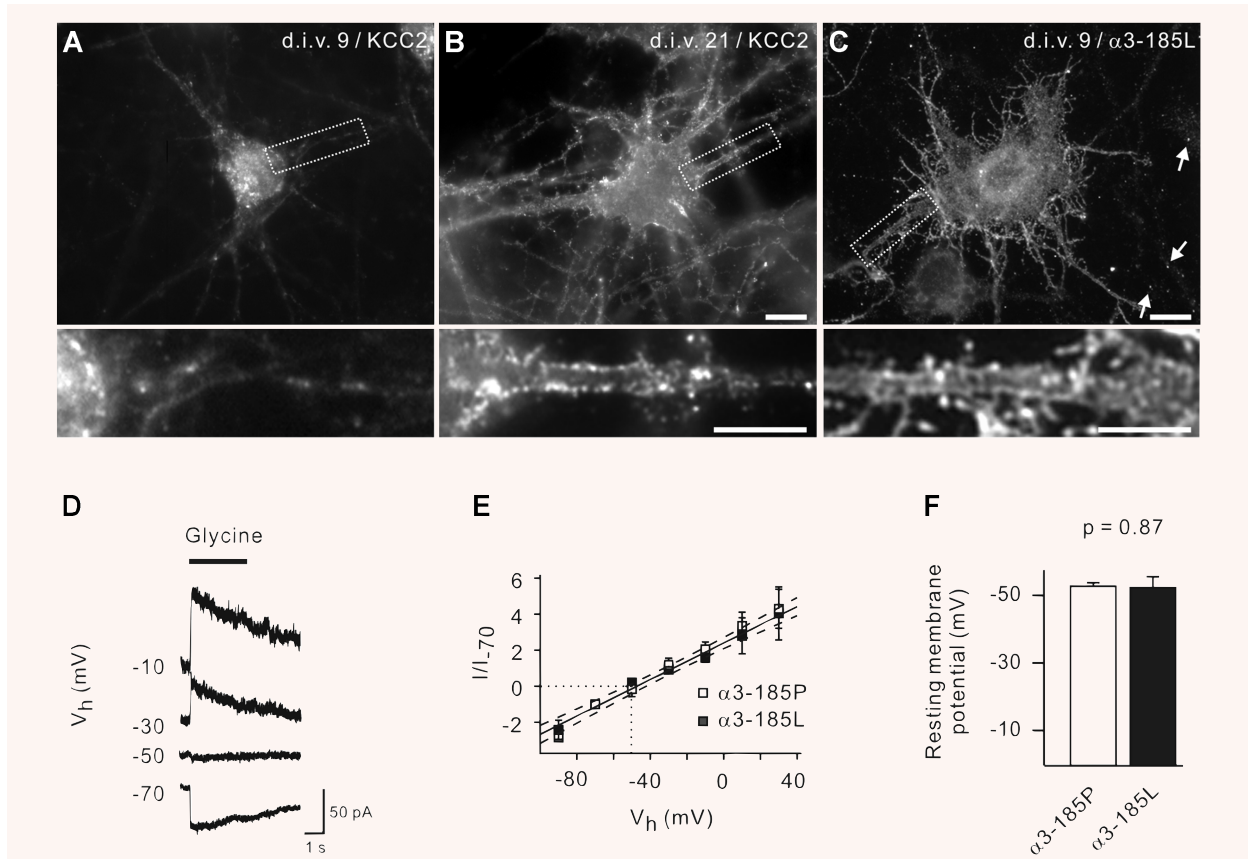
Fig. 2 Determination of the Cl⁻ equilibrium potential in primary rat hippocampal neurons. (**A**, **B**) Hippocampal neurons at d.i.v. 9 have reduced endogenous KCC2 expression, compared with mature neurons (**B**) at d.i.v. 21. (**C**) Uniform distribution of haGlyR $\alpha 3^{185L}$ over the somatodendritic compartment of a hippocampal neuron at d.i.v. 9. (**D**) Sample traces elicited with 100 μM glycine at different holding potentials, recorded in the perforated patch clamp configuration from a hippocampal neuron expressing haGlyR $\alpha 3^{185L}$. (**E**, **F**) Cl⁻ equilibrium potentials (**E**) and resting membrane potentials (**F**) in neurons expressing $\alpha 3^{185P}$ or $\alpha 3^{185L}$. Note the high and similar Cl⁻ equilibrium potentials in neurons expressing GlyR $\alpha 3^{185P}$ or $\alpha 3^{185L}$, which is in agreement with reduced endogenous KCC2 expression. Scale bars: 10 μm, and 5 μm in high power views.

Tonic inhibition by haGlyRs suppresses spontaneous Ca²⁺ transients and AP firing in hippocampal neurons with a high Cl⁻ equilibrium potential

To investigate potential effects of inverse regulation of KCC2 and haGlyR expression at a cellular, neuronal level, we developed an *in vitro* cell culture system utilizing selective activation of haGlyRs in hippocampal neurons with a high Cl⁻ equilibrium potential. Therefore, hippocampal neurons were chosen for investigation at d.i.v. 9, when the Cl⁻ equilibrium potential was still high (Fig. 2A, B, D and E). Neurons were transfected with DNAs encoding either haGlyR $\alpha 3^{185L}$ or low-affinity GlyR $\alpha 3^{185P}$; the latter served as a control throughout all experiments. The micrograph of Fig. 2C illustrates the uniform distribution of GlyR $\alpha 3^{185L}$ within the plas-

ma membrane of a transfected neuron at d.i.v. 9. From the intensity of the immunolabel we estimated $\alpha 3^{185L}$ expression to roughly correspond to that of endogenous GlyRs, visible as clusters in the vicinity of the transfected neuron (arrows). During GlyR $\alpha 3^{185L}$ expression, neurons were kept in the presence of 5 μM glycine, which corresponds to the formerly determined EC$_{50}$ of haGlyR $\alpha 3^{185L}$ [17] and which approximates hippocampal ambient glycine in TLE patients [16].

Gramicidin-perforated patch clamp recordings were performed to estimate the driving force for Cl⁻ ions in these hippocampal neurons (Fig. 2D and E). Neurons expressing $\alpha 3^{185P}$ or $\alpha 3^{185L}$ exhibited equal Cl⁻ reversal potentials (E$_{Cl}$ [mV]: $\alpha 3^{185P}$: -46.4 ± 0.8; $\alpha 3^{185L}$: -46.3 ± 1.2; Fig. 2E). In both cases, the difference between E$_{Cl}$ and the resting membrane potential (V$_m$) measured in the presence of 5 μM glycine amounted to 7–8 mV (V$_m$ [mV]: $\alpha 3^{185P}$: -53.6 ± 1.3; $\alpha 3^{185L}$: -54.5 ± 3.1, Fig. 2F).
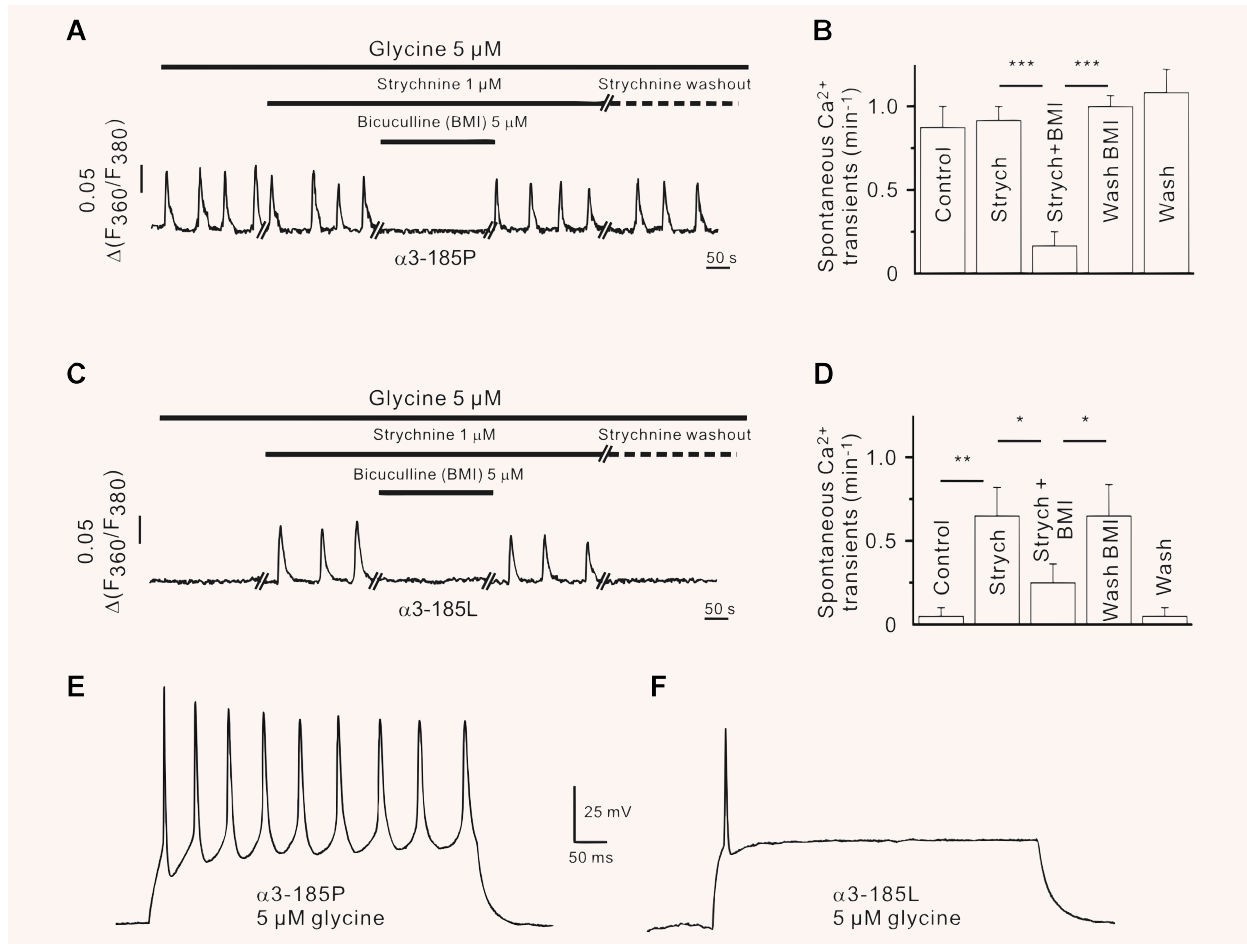
Fig. 3 haGlyRs and GABA$_A$Rs differentially modulate spontaneous activity of neurons with a high Cl$^-$ equilibrium potential. (**A–D**) Effect of 5 μM glycine on spontaneous Ca^{2+} transients in neurons expressing α3^{185P} (**A, B**) or α3^{185L} (**C, D**). Bicuculline methiodide (BMI) was used to block GABA$_A$Rs. Note the strychnine-mediated reversible relief of α3^{185L}-positive neurons from suppression of spontaneous Ca^{2+} transients. (**E, F**) In current clamp experiments, neurons expressing α3^{185P} (**E**) generate AP trains upon suprathreshold depolarization, while neurons with α3^{185L} (**F**) fire 1–2 APs only (see Table 2 for values). Error bars indicate the S.E.M. of the mean values obtained from at least three independent experiments. Significance levels are $P < 0.05$ (*), $P < 0.01$ (**) and $P < 0.001$ (***).

Furthermore, control and haGlyR α3^{185L}-expressing neurons were comparable with regard to Ca^{2+} levels at rest, measured in the presence of 5 μM glycine (F$_{360}$/F$_{380}$: α3^{185P}: 0.272 $\pm$ 0.004; α3^{185L}: 0.278 $\pm$ 0.005, $P = 0.3$).

To find out how glycine and GABA would affect spontaneous activity of the transfected neurons, spontaneous Ca^{2+} transients were recorded (Fig. 3A and C). This approach ensured preservation of the internal cellular milieu. Control neurons expressing low-affinity GlyR α3^{185P} were found to be spontaneously active in the presence of 5 μM glycine. They displayed no change associated with strychnine application, but were inhibited by 5 μM bicuculline methiodide (Ca^{2+} transients [per minute], α3^{185P}: 0.87 $\pm$ 0.13; α3^{185P} strychnine and bicuculline: 0.17 $\pm$ 0.08,

$P < 0.001$, paired Student's t-test; Fig. 3A and B). These results suggest that the controls lacked tonic glycinergic inhibition and responded to GABA with depolarization. In contrast, neurons expressing haGlyR α3^{185L} were not spontaneously active in the presence of 5 μM glycine and responded to strychnine application with disinhibition (Ca^{2+} transients [per minute], α3^{185L}: 0.05 $\pm$ 0.05; α3^{185L} strychnine: 0.65 $\pm$ 0.17, $P < 0.01$, paired Student's t-test; Fig. 3C and D). Bicuculline was shown to inhibit spontaneous activity, but, naturally in haGlyR α3^{185L}-expressing neurons, this suppressive effect could only be seen against the background of strychnine-induced disinhibition (Ca^{2+} transients [per minute], α3^{185L} strychnine: 0.65 $\pm$ 0.17; α3^{185L} strychnine and bicuculline: 0.25 $\pm$ 0.11,

Table 2 AP characteristics in control and activity-deprived neurons

	$\alpha3-185P$ ($n = 12$)	$\alpha3-185L$ ($n = 9$)	P
Amplitude (mV)	66.8 ± 1.6	54.6 ± 5.8	< 0.05
Threshold (mV)	40.1 ± 1.4	39.3 ± 1.3	> 0.7
Duration (ms)	4.6 ± 0.2	6.1 ± 0.5	< 0.01
APs (n/500 ms)	8.7 ± 0.7	1.8 ± 0.4	< 0.00001

$P < 0.05$, paired Student's t-test; Fig. 3C and D). Therefore, although both glycine and GABA open Cl^- channels, their effect on network activity is different, with GABA$_A$Rs eliciting spontaneous Ca^{2+} transients and haGlyRs inhibiting their appearance. Accordingly, whole-cell patch clamp recordings revealed that haGlyR-expressing neurons fired 1–2 APs upon suprathreshold depolarization, while control neurons answered adequate depolarization with a train of APs (Fig. 3E and F, Table 2). Thus, tonic activation of haGlyR by low glycine (in the range of hippocampal ambient glycine) strongly attenuates neuronal activity, even in hippocampal neurons with depolarizing GABAergic currents.

haGlyR activation shunts excitatory inputs

To elucidate the mechanisms underlying the differential effects of GABA and glycine on spontaneous neuronal activity, membrane resistance (R_m) and C_m were measured in the whole-cell configuration. Inhibited hippocampal neurons indeed displayed a decreased R_m in the presence of 5 μM glycine, while C_m was similar in both control and haGlyR $\alpha3^{185L}$-expressing neurons (R_m [MΩ]: $\alpha3^{185P}$: 493 ± 79; $\alpha3^{185L}$: 180 ± 25, $P < 0.01$; C_m [pF]: $\alpha3^{185P}$: 49 ± 6; $\alpha3^{185L}$: 44 ± 5, $P = 0.56$). In the whole-cell mode the resting potential of haGlyR $\alpha3^{185L}$-expressing neurons registered 10 min after break-through was significantly more positive (V_m [mV]: -35 ± 2 mV) than that of $\alpha3^{185P}$-expressing cells (V_m [mV]: -52 ± 1 mV, $P < 0.001$, unpaired Student's t-test). Because the intrapipette solution contained 50 mM Cl^-, which sets the Nernst equilibrium potential for Cl^- at about -20 mV, haGlyR activation by 5 μM glycine may underlie the observed shift of the resting potential. Indeed, application of strychnine shifted the resting potential in haGlyR $\alpha3^{185L}$-expressing cells to more negative values (V_m [mV]: -49 ± 3) but failed to affect $\alpha3^{185P}$-expressing cells (V_m [mV]: -53 ± 3). Therefore, given that hippocampal GABA$_A$Rs are clustered at synaptic sites [35] and that hippocampal GlyRs are apparently not involved in synaptic transmission [5, 6, 8], one can attribute the contrasting actions of GABA and glycine to synaptic GABA$_A$R-mediated excitation and tonic haGlyR-mediated shunt inhibition.

haGlyR-mediated tonic inhibition increases the Glu/GABA ratio of synaptic input through activation of iGluRs and TrkB receptors

As the frequency of spontaneous Ca^{2+} transients was slightly decreased in disinhibited haGlyR $\alpha3^{185L}$-positive neurons (Ca^{2+} transients [per minute], $\alpha3^{185P}$ strychnine: 0.92 ± 0.08; $\alpha3^{185L}$ strychnine: 0.65 ± 0.17, $P = 0.17$, Fig. 3B and D), while a slight increase in the frequency of spontaneous Ca^{2+} transients in haGlyR $\alpha3^{185L}$-expressing neurons could be observed in case both GABA$_A$Rs and GlyRs were blocked (Ca^{2+} transients in the presence of bicuculline and strychnine [per minute], $\alpha3^{185P}$: 0.17 ± 0.08; $\alpha3^{185L}$: 0.25 ± 11, $P = 0.55$; Fig. 3B and D), the synaptic connectivity pattern of haGlyR $\alpha3^{185L}$-expressing neurons may have changed in response to activity deprivation. To investigate this possibility, control and haGlyR $\alpha3^{185L}$-expressing neurons were immunolabelled with presynaptic markers for glutamatergic and GABAergic synapses.

The haGlyR $\alpha3^{185L}$-positive neurons were indeed found to receive more glutamatergic (VGluT$^+$ terminals, $\alpha3^{185P}$: 147 ± 6; $\alpha3^{185L}$: 201 ± 7) and less GABAergic terminals (VGAT$^+$ terminals, $\alpha3^{185P}$: 83 ± 3; $\alpha3^{185L}$: 52 ± 2), quantified within a circular ROI (diameter: 100 μm) projected on the somatodendritic compartment (Fig. 4A–D). The number of glutamatergic and GABAergic terminals was correlated (Fig. 4E), suggesting that the Glu/GABA ratio is kept within a narrow range [36] irrespective of the total number of presynaptic terminals a single neuron receives. However, Glu/GABA ratios extracted from activity-deprived, haGlyR $\alpha3^{185L}$-expressing neurons were increased (Figs 4E, F and 5A).

To substantiate this morphological data, miniature postsynaptic currents were recorded (Fig. 4G and H). As described previously [30], glutamatergic and GABAergic miniature postsynaptic currents (mEPSC, mIPSC) were distinguished by their decay kinetics. Both, mEPSC and mIPSC were detected in all control neurons ($n = 12$). Based on their frequencies, the Glu/GABA ratio of synaptic input was determined for each recorded cell (mEPSC/mIPSC, $\alpha3^{185P}$: 0.75 ± 0.21). The discrepancy between the Glu/GABA ratios obtained from morphological and electrophysiological analysis suggests the presence of a fraction of morphologically but not yet functionally established synapses, which is characteristic for a developing network [37]. In contrast, only a few (three of nine) haGlyR $\alpha3^{185L}$-positive neurons displayed mIPSCs, which occurred at one out of three of the frequency of control neurons. However, not any mEPSC could be extracted from these recordings, most likely because neuronal membranes containing activated haGlyR $\alpha3^{185L}$ channels filter out all fast mEPSCs.

We know from previous studies that activation of ionotropic glutamate receptors (iGluRs) and tyrosine kinase B (TrkB) receptors contribute to the regulation of Glu/GABA ratios of synaptic input [30]. Moreover, it was shown that brain-derived neurotrophic factor (BDNF) expression increases in epileptic hippocampi [34] and causes down-regulation of KCC2 [18–20, 34]. Therefore, we applied DNQX/MK801 and K252a to block iGluRs and TrkB

Fig. 4 Tonic GlyR $\alpha3^{185L}$ activation by 5 μM glycine increases the Glu/GABA ratio of synaptic input to hippocampal neurons with a high Cl^- equilibrium potential. (**A**, **B**) Representative images of hippocampal neurons expressing either $\alpha3^{185P}$ or $\alpha3^{185L}$ (blue). VGAT and VGluT immunoreactivities are represented in red and green colours, respectively. (**C**, **D**) Quantification of the number of VGluT and VGAT immunoreactive (+) terminals in contact with neurons expressing $\alpha3^{185P}$ or $\alpha3^{185L}$. (**E**) The number of VGluT$^+$ and VGAT$^+$ terminals in contact with neurons expressing $\alpha3^{185P}$ (open circles) or $\alpha3^{185L}$ (filled circles) are correlated. (**F**) Histogram illustrating Glu/GABA ratio distributions in neurons expressing $\alpha3^{185P}$ or $\alpha3^{185L}$. (**G**, **H**) Miniature glutamatergic and GABAergic postsynaptic currents recorded from a neuron expressing $\alpha3^{185P}$. Error bars indicate the S.E.M. of the mean values obtained from at least three independent experiments. Significance level is $P < 0.001$ (***). Scale bar: 10 μm, high power views: 5 μm.
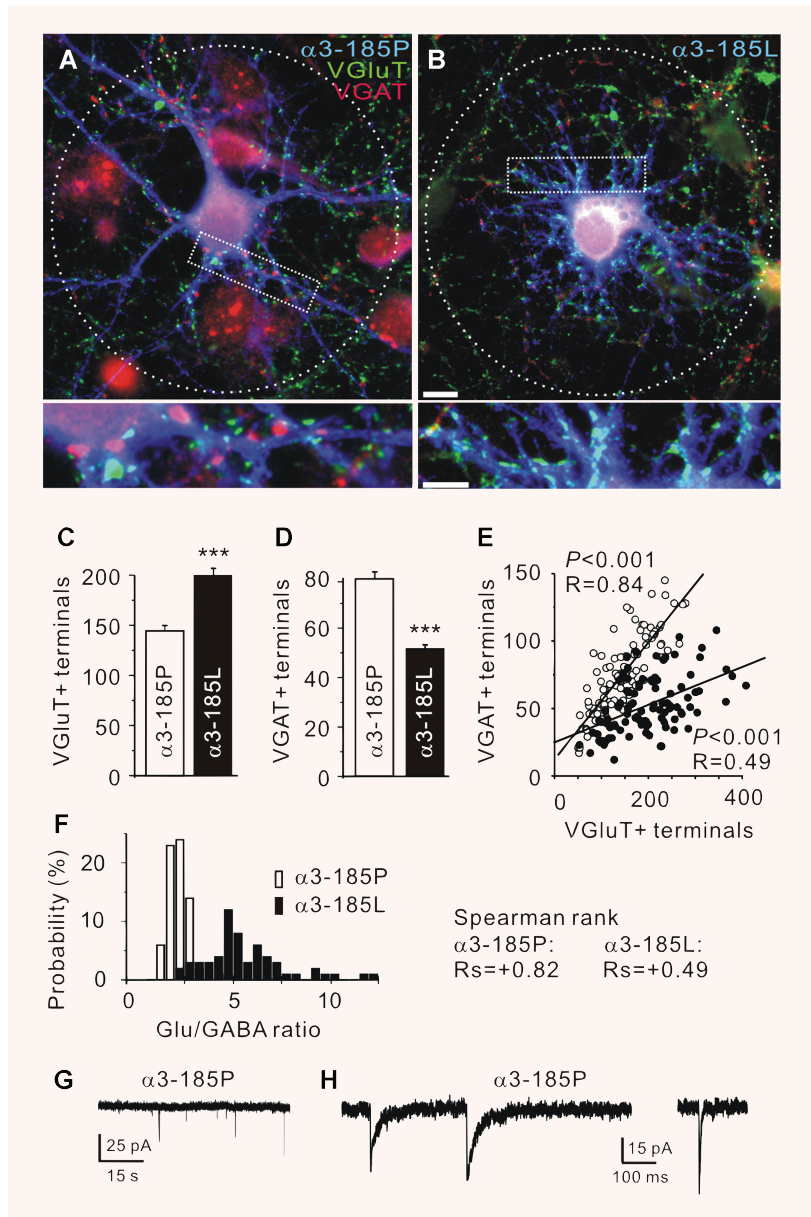
receptors, respectively, during haGlyR $\alpha3^{185L}$ expression in neurons with a high Cl^- equilibrium potential. Indeed, Glu/GABA ratios were rescued in the presence of iGluR and TrkB receptor antagonists (Fig. 5A, see Table 3 for values). When iGluR activation was prohibited with DNQX and MK801 (Fig. 5B and C), haGlyR $\alpha3^{185L}$-expressing neurons were still contacted by more glutamatergic terminals (VGluT$^+$ terminals [% of $\alpha3^{185P}$]: 149 $\pm$ 7), but loss of GABAergic terminals was entirely prevented (VGAT$^+$ terminals [% of $\alpha3^{185P}$]: 95 $\pm$ 5). In control neurons, iGluR blockade had no effect on GABAergic terminals (VGAT$^+$ terminals [% of $\alpha3^{185P}$]: 96 $\pm$ 9) but, in agreement with the concept of

homeostatic regulation [38], increased the number of glutamatergic synapses (VGluT$^+$ terminals [% of $\alpha3^{185P}$]: 125 $\pm$ 8).

In line with previous data [30], TrkB receptor blockade (Fig. 5D and E) was not only capable of rescuing GABAergic synapses in contact with $\alpha3^{185L}$-positive neurons but increased their number beyond the control level (VGAT$^+$ terminals [% of $\alpha3^{185P}$]: 120 $\pm$ 4). Gain in GABAergic terminals was also evident in $\alpha3^{185P}$-expressing control neurons (VGAT$^+$ terminals [% of $\alpha3^{185P}$]: 118 $\pm$ 4). As for the experiments with DNQX/MK801, K252a up-regulated the number of glutamatergic terminals in both $\alpha3^{185L}$-expressing (VGluT$^+$ terminals [% of $\alpha3^{185P}$]: 163 $\pm$ 3) and control neurons (VGluT$^+$ terminals
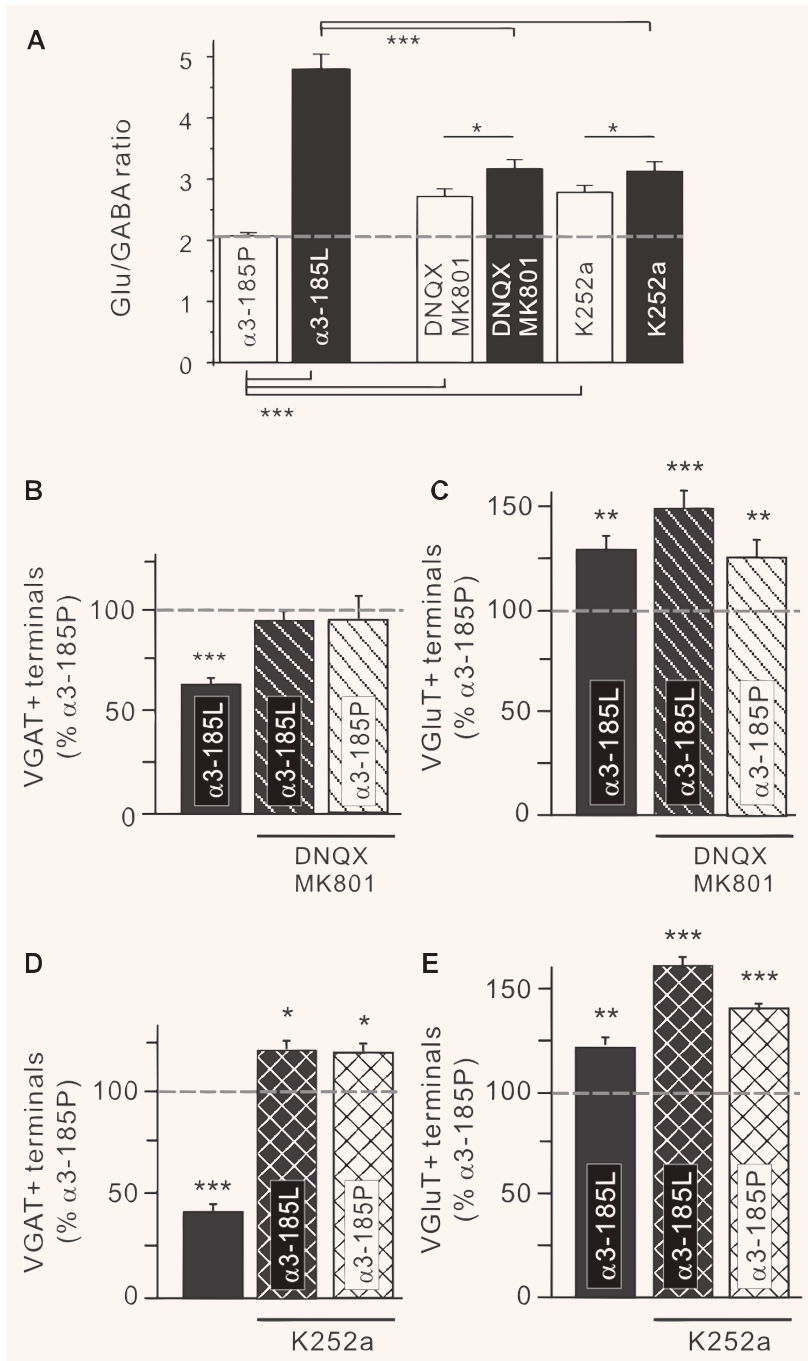
Fig. 5 Activity-dependent regulation of GABAergic synapses in hippocampal neurons with a high Cl⁻ equilibrium potential. (**A**) Glu/GABA ratios obtained from neurons treated with iGluR or TrkB receptor antagonists during $\alpha3^{185P}$ or $\alpha3^{185L}$ receptor expression. See Table 3 for values. Blockade of iGluRs (**B**, **C**) or TrkB receptors (**D**, **E**) rescues $\alpha3^{185L}$-expressing neurons from down-regulation of the number of VGAT⁺ terminals. Note that the TrkB receptor antagonist K252a increases the number of VGAT⁺ terminals beyond control levels. Also note that the number of VGluT⁺ terminals was up-regulated in case of iGluR and TrkB receptor blockade, irrespective of the receptor variant expressed. Error bars indicate the S.E.M. of the mean values obtained from at least three independent experiments. Significance levels are $P < 0.05$ (*), $P < 0.01$ (**) and $P < 0.001$ (***).

[% of $\alpha3^{185P}$]: 143 $\pm$ 2). Therefore, Glu/GABA ratios of synaptic input to K252a-treated neurons were similar to those extracted from DNQX/MK801-supplemented cultures (Fig. 5A, Table 3).

In conclusion, we propose that down-regulation of GABAergic terminals in contact with inhibited, haGlyR $\alpha3^{185L}$-positive hippocampal neurons occurs secondarily to up-regulation of glutamatergic terminals and is mediated by iGluRs and TrkB receptors.

iGluR and TrkB receptor activation reduces dendrite length of inhibited hippocampal neurons

Quantification of the number of dendrites exceeding 50 μm (Fig. 6A) revealed reduced dendrite length of neurons with haGlyR $\alpha3^{185L}$ (dendrites > 50 μm, $\alpha3^{185P}$: 10.2 $\pm$ 0.4; $\alpha3^{185L}$: 7.0 $\pm$ 0.6). Because previous studies showed that dendrite elongation is

Table 3 Effects of iGluR and TrkB receptor antagonists on Glu/GABA ratios of synaptic input to neurons expressing $\alpha3^{185P}$ or $\alpha3^{185L}$

|	—	DNQX / MK801	K252a
$\alpha3^{185P}$	2.08 ± 0.05	2.72 ± 0.12	2.79 ± 0.11
$\alpha3^{185L}$	4.81 ± 0.24	3.17 ± 0.15	3.13 ± 0.15

negatively regulated by glutamatergic input [30, 39], and considering our observation of increased Glu/GABA ratios of synaptic input to haGlyR $\alpha3^{185L}$-expressing hippocampal neurons, increased glutamatergic signalling may have been responsible for reduction of dendrite length. The fact that we found the number of glutamatergic terminals and the number of dendrites exceeding 50μm length to be inversely correlated (Fig. 6B) further argues in favour of this possibility. Furthermore, as it is known that TrkB receptor activation is capable of reducing dendrite length [30], we analyzed the ability of both iGluR and TrkB receptor blockades to reverse $\alpha3^{185L}$-associated reduction of dendrite length (Fig. 6C and D). Both iGluR and TrkB receptor antagonists were indeed effective in preventing reduction of dendrite length (dendrites > 50 μm [% of $\alpha3^{185P}$]: $\alpha3^{185L}$: 45 ± 4, $\alpha3^{185L}$ + DNQX/MK801: 105 ± 5; $\alpha3^{185L}$: 29 ± 3, $\alpha3^{185L}$ + K252a: 108 ± 5). Actually, iGluR antagonists further increased the number of dendrites exceeding 50 μm beyond the control level (dendrites > 50 μm [% of $\alpha3^{185P}$]: $\alpha3^{185P}$ + DNQX/MK801: 117 ± 6; $\alpha3^{185P}$ + K252a:

104 ± 3), presumably revealing a steady control of dendrite length by iGluR activation in these cultures. Therefore, reduced dendrite length in neurons with haGlyR $\alpha3^{185L}$ is interpreted to occur as a consequence of elevated glutamatergic signalling.

haGlyR-mediated tonic inhibition increases neuronal susceptibility to excitotoxicity

The fact that haGlyR $\alpha3^{185L}$-expressing hippocampal neurons shifted their Glu/GABA ratios in favour of glutamatergic terminals and that elevated glutamatergic signalling was involved in reduction of dendrite length suggested that these neurons were more susceptible to cell death. To systematically investigate this possibility, we first analysed caspase-3 activation in both control ($\alpha3^{185P}$) and haGlyR $\alpha3^{185L}$-positive neurons. Neurons were cotransfected with GlyRs and the reporter construct caspase-3 sensor, which utilizes the activated caspase-3 consensus cleavage site DEVD for secession of a nuclear exclusion sequence (NES) [25, 40]. Upon NES cleavage by activated caspase-3, the reporter protein EYFP is translocated into the nucleus (Fig. 7A) with the aid of the remaining nuclear localization sequence. Accordingly, nuclear exclusion of the EYFP reporter protein indicates reduced or absent caspase-3 activation (Fig. 7B). Using this reporter construct, we found that both control and $\alpha3^{185L}$-positive neurons exhibited similar caspase-3 activation, expressed as percentages of GlyR-expressing neurons with nuclear caspase-3 sensor (Fig. 7C, days after transfection: dpt). Furthermore, in both control

Fig. 6 Activity-dependent regulation of dendrite length of hippocampal neurons with a high Cl⁻ equilibrium potential. (**A**) The number of dendrites longer than 50 μm is shown for control and GlyR $\alpha3^{185L}$-expressing hippocampal neurons. (**B**) Inverse correlation between the number of VGluT⁺ terminals and the number of dendrites longer than 50 μm. (**C**, **D**) Effects of iGluR and TrkB receptor antagonists on dendrite length. Note that dendrite length is restored upon blockade of iGluRs or TrkB receptors. Also note that iGluR blockade increased the number of dendrites exceeding 50 μm beyond the control level. Error bars indicate the S.E.M. of the mean values obtained from at least three independent experiments. Significance levels are $P < 0.05$ (*) and $P < 0.001$ (***).
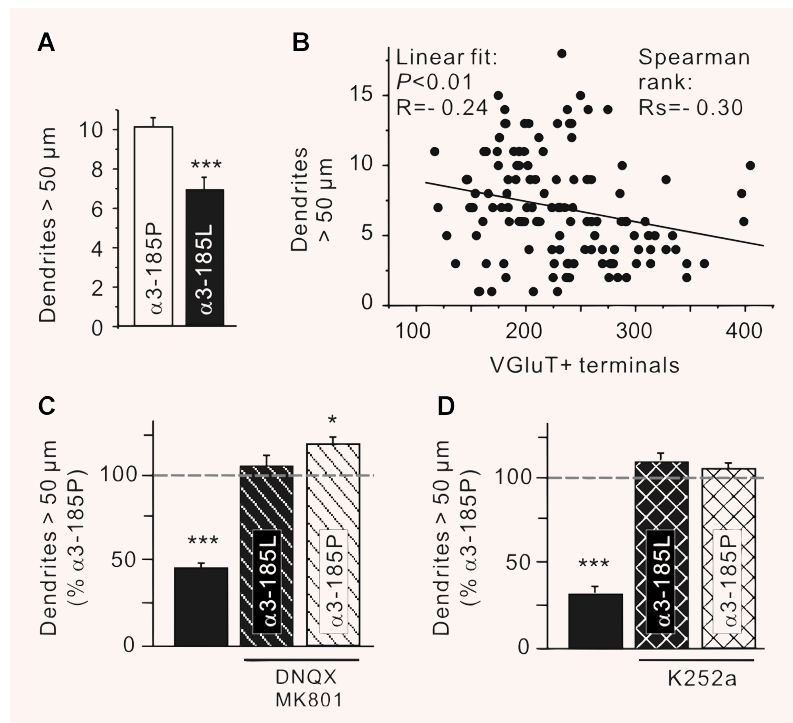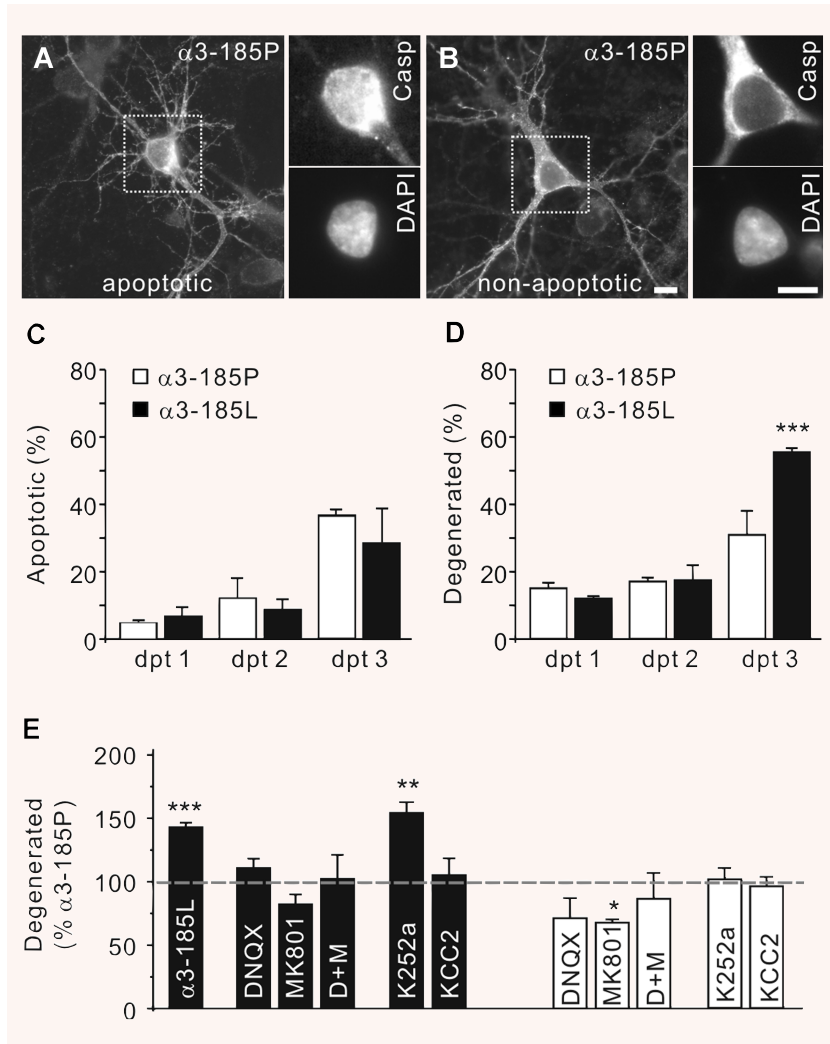
Fig. 7 Inhibited hippocampal neurons with a high Cl⁻ equilibrium potential undergo excitotoxicity. (**A**, **B**) Images show apoptotic (**A**, nuclear caspase-3 sensor enrichment) and non-apoptotic (**B**, nuclear caspase-3 sensor exclusion) control neurons. (**C**) Quantification of the percentages of apoptotic neurons at different time-points after transfection (days after transfection, dpt). (**D**) Quantification of the percentages of morphologically identified degenerated neurons, according to the presence of dendrite fragmentation and dendritic swellings. Note that a significant fraction of degenerated neurons is attributable to haGlyR $\alpha 3^{185L}$ expression. (**E**) Pharmacological profiles of degeneration of neurons expressing haGlyR $\alpha 3^{185L}$ or GlyR $\alpha 3^{185P}$. Note that blockade of iGluRs or KCC2 cotransfection rescues inhibited neurons, while blockade of TrkB receptors is ineffective. D: DNQX, M: MK801. Error bars indicate the S.E.M. of the mean values obtained from at least three independent experiments. Significance levels are $P < 0.05$ (*), $P < 0.01$ (**) and $P < 0.001$ (***). Scale bars: 10 μm.

and $\alpha 3^{185L}$-positive neurons nuclear enrichment with caspase-3 sensor delineated a similar time course after transfection (neurons with nuclear caspase-3 sensor [%], $\alpha 3^{185P}$: dpt 1: 5 ± 1, dpt 2: 12 ± 6, dpt 3: 37 ± 2; $\alpha 3^{185L}$: dpt 1: 7 ± 3, dpt 2: 9 ± 3, dpt 3: 28 ± 10; Fig. 7C). Because the percentages of neurons with activated caspase-3 were similar in both control and haGlyR $\alpha 3^{185L}$-positive neurons, we conclude that caspase-3 activation occurred as a result of the transfection procedure.

However, according to the appearance of fragmented dendrites and dendritic swellings, an additional fraction of degenerating neurons was clearly attributable to haGlyR $\alpha 3^{185L}$ expression three days after transfection (Fig. 7D; fraction of neurons with dendrite fragmentation and dendritic swellings [%], $\alpha 3^{185P}$: dpt 1: 15 ± 1, dpt 2: 17 ± 1, dpt 3: 31 ± 7; $\alpha 3^{185L}$: dpt 1: 12 ± 1, dpt 2: 18 ± 4, dpt 3: 56 ± 1). Because our results so far point to elevated glutamatergic signalling as an executive mechanism of haGlyR $\alpha 3^{185L}$-mediated activity deprivation, we investigated the

potential of iGluR antagonists to rescue hippocampal neurons. Indeed, blockade of iGluRs with DNQX or MK801 rescued inhibited hippocampal neurons from degeneration (fraction of neurons with dendrite fragmentation and dendritic swellings at 3 dpt [% of $\alpha 3^{185P}$]: $\alpha 3^{185L}$ + DNQX: 111 ± 7, $\alpha 3^{185L}$ + MK801: 83 ± 7). However, a combined blockade of AMPA and NMDA receptors was not additive, neither in haGlyR $\alpha 3^{185L}$-positive nor in control neurons (fraction of neurons with dendrite fragmentation and dendritic swellings at 3 dpt [% of $\alpha 3^{185P}$]: $\alpha 3^{185P}$ + DNQX + MK801: 86 ± 20; $\alpha 3^{185L}$ + DNQX + MK801: 103 ± 18).

As iGluR antagonists also restored GABAergic terminals, it remained to be clarified whether recovery of GABAergic terminals would rescue inhibited neurons. Because of their capacity to restore GABAergic terminals, TrkB receptors were blocked during haGlyR expression. Irrespective of the GlyR variant expressed, K252a had no effect on neuron survival (fraction of neurons with dendrite fragmentation and dendritic swellings at 3 dpt [% of

Fig. 8 Decrease of the Cl$^-$ equilibrium potential by KCC2 expression restores GABAergic synapses and Glu/GABA ratios. (**A**, **B**) VGAT$^+$ and VGluT$^+$ terminal counts obtained from hippocampal neurons expressing $\alpha3^{185P}$ or $\alpha3^{185L}$, each alone or in combination with KCC2. (**C**) Resulting Glu/GABA ratios. (**D**) Number of dendrites exceeding 50 μm. Note that the decrease of the Cl$^-$ equilibrium potential by KCC2 expression reverses the adverse effects of tonic inhibition of hippocampal neurons, except dendrite length. Also note that KCC2 expression increased the number of VGAT$^+$ terminals beyond control level in both control and haGlyR $\alpha3^{185L}$-expressing neurons, while the number of VGluT$^+$ terminals remained up-regulated in haGlyR $\alpha3^{185L}$-expressing neurons. Error bars indicate the S.E.M. of the mean values obtained from at least three independent experiments. Significance levels are $P < 0.01$ (**) and $P < 0.001$ (***).
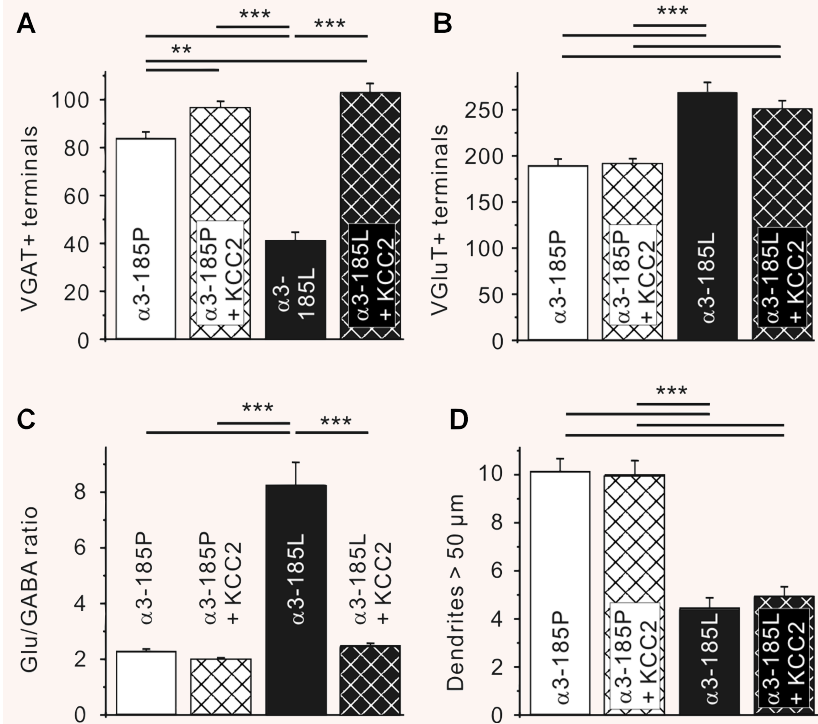

$\alpha3^{185P}$]: $\alpha3^{185L}$ + K252a: 154 $\pm$ 8, $\alpha3^{185P}$ + K252a: 102 $\pm$ 9). Therefore, we can rule out the possibility that down-regulation of GABAergic terminals contributed to haGlyR $\alpha3^{185L}$-elicited neuron degeneration. Altogether, we conclude that the enhanced susceptibility of haGlyR $\alpha3^{185L}$-expressing neurons to degeneration reflects excitotoxicity mediated by iGluRs.

A decrease of Cl$^-$ equilibrium potential by KCC2 expression rescues hippocampal neurons and Glu/GABA ratios

The results presented so far were obtained from hippocampal neurons with a high Cl$^-$ equilibrium potential. Because KCC2 down-regulation is known to cause a high Cl$^-$ equilibrium potential in TLE hippocampal neurons [18–20], we examined whether decreasing the Cl$^-$ equilibrium potential by KCC2 cotransfection with haGlyRs would restore Glu/GABA ratios of synaptic input, dendrite length and survival. KCC2 expression in cotransfection experiments indeed had the capacity to rescue hippocampal neurons from excitotoxicity (Fig. 7E; fraction of neurons with dendrite fragmentation and dendritic swellings at 3 dpt [% of $\alpha3^{185P}$]: $\alpha3^{185P}$ + KCC2: 96 $\pm$ 7, $\alpha3^{185L}$ + KCC2: 106 $\pm$ 13).

Decreasing the Cl$^-$ equilibrium potential by KCC2 cotransfection also restored GABAergic terminals in contact with haGlyR $\alpha3^{185L}$-positive neurons (Fig. 8A; VGAT$^+$ terminals: $\alpha3^{185L}$: 41 $\pm$ 3; $\alpha3^{185L}$ + KCC2: 103 $\pm$ 4), even in the context of elevated glutamatergic innervation (Fig. 8B; VGluT$^+$ terminals: $\alpha3^{185L}$: 269 $\pm$ 10; $\alpha3^{185L}$ + KCC2: 251 $\pm$ 9). In fact, KCC2 expression increased the number of GABAergic terminals in contact with inhibited neurons beyond the control level. Furthermore and in agreement with previous data [41], even control neurons that were cotransfected with KCC2 received more GABAergic terminals (Fig. 8A; VGAT$^+$ terminals: $\alpha3^{185P}$ + KCC2: 96 $\pm$ 3; $\alpha3^{185L}$ + KCC2: 103 $\pm$ 4 *versus* $\alpha3^{185P}$: 84 $\pm$ 3). Therefore, decreasing the Cl$^-$ equilibrium potential by KCC2 cotransfection was sufficient to also restore Glu/GABA ratios of synaptic input (Fig. 8C; Glu/GABA ratio: $\alpha3^{185L}$: 8.3 $\pm$ 0.8; $\alpha3^{185L}$ + KCC2: 2.5 $\pm$ 0.1 *versus* $\alpha3^{185P}$: 2.3 $\pm$ 0.08), again even in the context of elevated glutamatergic innervation.

In conclusion, a decrease of the Cl$^-$ equilibrium potential by KCC2 expression reversed all adverse effects associated with haGlyR $\alpha3^{185L}$ expression except dendrite length (Fig. 8D; dendrites > 50 μm: $\alpha3^{185L}$: 4.5 $\pm$ 0.4; $\alpha3^{185L}$ + KCC2: 4.9 $\pm$ 0.4), which remained reduced – most likely due to persistently increased glutamatergic innervation (Figs. 6 and 8B).
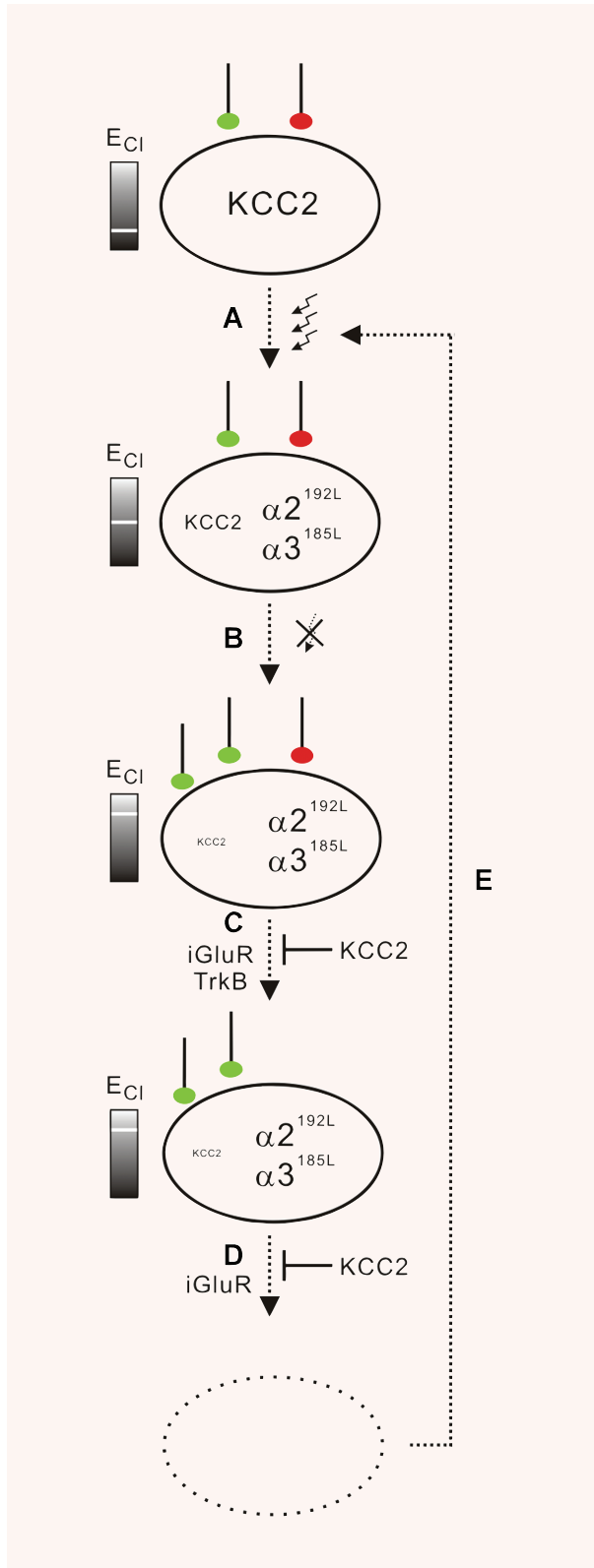
Discussion

The main findings of this study support the conclusion that suppression of spontaneous activity of hippocampal neurons with reduced KCC2 expression and a high Cl⁻ equilibrium potential elicits TLE histopathological characteristics, in terms of elevated Glu/GABA ratios of synaptic input, reduced dendrite length and elevated susceptibility of hippocampal neurons to excitotoxicity [1, 2, 42, 43]. Accordingly, our study revealed elevated expression of high-affinity type GlyR $\alpha2$ and $\alpha3$ in hippocampectomies of TLE patients with a severe course of disease, according to the Wyler classification [21] of hippocampal sclerosis or the frequency of SGTCS. In addition, GlyR $\alpha2B$ [13] expression was found to be elevated in these patients. Finally, in TLE patients, increased haGlyR expression inversely correlated with KCC2 expression. On the basis of these complementary results, obtained from primary hippocampal neurons and from TLE patients, we suggest a scenario that implicates elevated haGlyR expression and consequently neuronal hypoactivity in the pathophysiology of TLE, provided that the neuronal Cl⁻ equilibrium potential is high (Fig. 9).

Human hippocampal neurons have the potential to generate haGlyR variants

We adapted the previously described method for quantification of haGlyR expression [17] to human *Glra2* and *Glra3* transcript sequences (Supplementary Fig. 1A) and validated this modified approach by calibration (Supplementary Fig. 1B). In addition, sequencing of genomic DNA ruled out the possibility that haGlyR

Fig. 9 Proposed scenario involving inverse regulation of haGlyR and KCC2 expression in the course of TLE. (**A**) Neuronal stressors, such as epileptic seizures, provoke activity-dependent down-regulation of KCC2, which raises the Cl⁻ equilibrium potential, and up-regulation of haGlyRs, which are capable of translating hippocampal ambient glycine into tonic inhibition. (**B**) Inhibited hippocampal neurons scale up their number of glutamatergic terminals (green), which drives down-regulation of KCC2 in a BDNF-dependent way. (**C**) In these neurons with high Cl⁻ equilibrium potentials, down-regulation of GABAergic contacts (red) involves iGluRs and TrkB receptor signalling. (**D**) Finally, still in the context of a high Cl⁻ equilibrium potential, hippocampal neurons with upscaled glutamatergic and downscaled GABAergic synaptic inputs become vulnerable to excitotoxicity. (**E**) Neuron degeneration contributes to further decreasing seizure threshold. Importantly, a decrease of the Cl⁻ equilibrium potential by KCC2 expression rescued inhibited hippocampal neurons from both iGluR- and TrkB receptor-dependent downscaling of GABAergic terminals and from excitotoxic degeneration.

$\alpha2^{575T}$ (examples given in Supplementary Fig. 1C) and haGlyR $\alpha3^{554T}$ (not shown) were of genomic origin. Thus, our results obtained from TLE patients provide evidence that GlyR C-to-U RNA editing is neither subunit nor species specific [17]. The affinities for glycine of RNA-edited $\alpha2A^{192L}$- and $\alpha2B^{192L}$-GlyRs are particularly high, allowing these receptors responding to submicromolar glycine levels (Supplementary Fig. 1D). Notably, haGlyR $\alpha2B^{192L}$ responds to 0.1 μM glycine with currents reaching ~15% of maximal current amplitudes (Supplementary Fig. 1D). Our data identified increased expression of GlyR $\alpha2B$ in W2–4 TLE patients, providing us with evidence to propose that human hippocampal cells have the potential to generate haGlyRs by alternative splicing of GlyR $\alpha2$ transcripts and by C-to-U editing of all types of hippocampal ligand binding GlyR α subunit mRNAs.

The affinity of haGlyRs approximates the level of hippocampal ambient glycine

Our hippocampal cell culture model system uses 5 μM glycine for selective activation of haGlyR $\alpha3^{185L}$ [17]. We have chosen this glycine concentration also because it corresponds to the level of seizure-related hippocampal ambient glycine measured in TLE patients [16]. However, considering the GlyT-1 stoichiometry of substrate/ion cotransport (2 Na^+/Cl^-/glycine) and the bi-directional character of GlyT-1 glycine transport, the level of hippocampal ambient glycine may actually be kept within the sub-micromolar range, which is optimal for functional modulation of NMDA-type glutamate receptors [44]. Nevertheless, given the voltage dependency of GlyT-1 glycine transport, it is conceivable that neuronal activity raises hippocampal ambient glycine to supramicromolar levels [15, 45], which may become particularly relevant when considering that neuronal high frequency activity is a precursor of recurrent epileptiform discharges [46]. Therefore, we consider the affinity of haGlyRs well suited for the translation of hippocampal ambient glycine into tonic inhibition, especially under conditions of sustained hippocampal network activity.

Thus, haGlyRs are functionally well adjusted for translation of hippocampal ambient glycine into tonic glycinergic inhibition, potentially providing a cellular basis for the recently uncovered hypoactivity of hippocampal neurons in cases of TLE [47, 48]. Although the time course of disease progression was heterogeneous in the TLE patients investigated here (see Table 1), elevated haGlyR expression occurred in a large fraction of patients with a severe course of disease or frequent SGTCS. This suggests that up-regulation of haGlyR expression may occur in response to neuronal stressors, such as aberrant high frequency activity [46], and that it persists in TLE patients beyond the initial insult. Altogether, our results suggest that haGlyRs are candidate molecules potentially contributing to the course of TLE by increasing tonic glycinergic inhibition, even in neurons with a high Cl^- equilibrium potential.

A hippocampal cell culture system for determination of the consequences of neuronal hypoactivity in the context of a high Cl^- equilibrium potential

We established a hippocampal cell culture system to characterize the potential consequences of elevated haGlyR expression in the context of reduced KCC2 expression and a high Cl^- equilibrium potential. For this purpose, we used hippocampal neurons at a developmental state when their Cl^- equilibrium potential was high, as is the case in TLE patients [20]. Furthermore, the glycine concentration present during GlyR expression approximated hippocampal ambient glycine measured in TLE patients [16] and selectively activated haGlyR $\alpha3^{185L}$ [17]. Importantly, both the suppression of spontaneous Ca^{2+} transients and AP generation by haGlyR activation renders our system suitable for elucidation of potential consequences of neuronal hypoactivity in the context of a high Cl^- equilibrium potential, which is characteristic for TLE [48]. Thereby, haGlyR activation likely shunts excitatory inputs because similar resting membrane potentials were measured in perforated patch clamp recordings, irrespective of the GlyR variant expressed. Furthermore, decreased membrane resistances and more positive membrane potentials were determined in the whole-cell configuration in neurons with activated haGlyRs. Finally, this system allowed us to investigate whether decreasing the Cl^- equilibrium potential would be sufficient to reverse the consequences of haGlyR $\alpha3^{185L}$-elicited neuronal hypoactivity.

Disequilibrated iGluR and TrkB receptor signalling constitute executive mechanisms of haGlyR $\alpha3^{185L}$-mediated tonic inhibition

The fact that the resting membrane potential and resting Ca^{2+} levels were not affected by haGlyR $\alpha3^{185L}$ expression indicates that the consequences of increased tonic glycinergic inhibition on hippocampal neurons were indirect. Indeed, all effects associated with haGlyR $\alpha3^{185L}$ activation were reversible upon application of iGluR antagonists. Because increased BDNF expression occurs in epileptic hippocampi [34] and causes down-regulation of KCC2 [18–20, 34], we additionally evaluated the potential of TrkB receptor blockade to rescue hippocampal haGlyR $\alpha3^{185L}$-expressing neurons, in the context of a high Cl^- equilibrium potential. According to these data, we propose that disequilibrated TrkB receptor [18, 34, 49] and iGluR signalling [1] account for the emergence of TLE-characteristic histopathological signs. Although our results do not allow for distinction between presynaptic [50] and postsynaptic [30] BDNF-release from glutamatergic synapses, they lend support to a convergent regulatory signalling pathway within the postsynaptic neuron [51]. However, the fact that TrkB receptor blockade was not sufficient to rescue hippocampal neurons from degeneration, and considering that antagonists of iGluRs or KCC2 expression were neuroprotective, accentuates the involvement of excitotoxicity. Because spontaneous

neuronal activity was mainly driven by GABA$_A$Rs in these hippocampal neurons, our results favour the possibility that excitotoxicity relied on activation of extrasynaptic iGluRs [52].

haGlyR $\alpha3^{185L}$-elicited effects are conditional upon a high Cl$^-$ equilibrium potential

In the mature nervous system neuronal activity-deprivation is compensated for by concomitant up-regulation of glutamatergic and GABAergic synapses [53]. However, reducing neuronal activity within a developing, immature neuronal network is known to cause loss of GABAergic synapses, which potentially reflects failure of synchronization of glutamatergic and GABAergic postsynaptic currents [54]. All the consequences of haGlyR $\alpha3^{185L}$-mediated tonic inhibition were obvious in neurons with a high Cl$^-$ equilibrium potential, which corresponds to an early developmental status of the neuronal network. Because the epileptic neuronal network is characterized by KCC2 down-regulation and, hence, depolarizing GABAergic currents [19], we analysed the potential of KCC2 expression to rescue hippocampal neurons. Decreasing the Cl$^-$ equilibrium potential by KCC2 expression indeed rescued Glu/GABA ratios in contact with inhibited neurons and, in addition, exerted neuroprotective effects. Although our data do not permit drawing conclusions on the underlying mechanisms, they highlight the deleterious aspect of enhanced tonic inhibition, which is conditional according to the Cl$^-$ equilibrium potential of inhibited neurons.

The fact that dendrite length was not restored upon decreasing the Cl$^-$ equilibrium potential by KCC2 expression may reflect persistently increased glutamatergic signalling to inhibited neurons, which is substantiated by the inverse correlation between the number of glutamatergic terminals and dendrite length that we and others [30] observed. In addition, this argumentation is in line with the formerly established concept of negative regulation of dendrite length by glutamatergic signalling [39]. Moreover, the possibility that loss of depolarising GABAergic terminals was responsible for reduced dendrite length was ruled out because KCC2 expression decreased the Cl$^-$ equilibrium potential, which did not further reduce dendrite length of inhibited neurons.

Activity-deprivation results in homeostatic but pathophysiological, structural reorganization reminiscent of TLE histopathology

Recently it was shown that activity deprivation leads to seizures in hippocampal slice cultures [55]. Our data are in agreement with this observation because it establishes a coherency between hypoactivity of hippocampal neurons with a high Cl$^-$ equilibrium potential and TLE-typical histopathological features. Moreover, we found elevated levels of haGlyR expression to be associated with hippocampal damage and the frequency of SGTCS. Furthermore, we provide evidence for the involvement of homeostatic, but pathophysiological, recruitment of iGluR and TrkB receptor signalling in the emergence of TLE-reminiscent histopathological features. In this regard, we would like to put forward a chain of events implicating inverse regulation of haGlyR and KCC2 expression in the course of TLE. According to the proposed scenario (Fig. 9), seizure activity triggers BDNF- and TrkB receptor-dependent down-regulation of KCC2 [18, 34] together with up-regulation of haGlyR expression (Fig. 9A). haGlyRs respond to hippocampal ambient glycine with tonic inhibition, and inhibited neurons upscale their number of presynaptic glutamatergic terminals (Fig. 9B). In the context of a high Cl$^-$ equilibrium potential, down-regulation of the number of GABAergic contacts then develops secondarily from increased glutamate- and BDNF-dependent signalling (Fig. 9C). Neurons with upscaled glutamatergic and downscaled GABAergic inputs become vulnerable to excitotoxicity (Fig. 9D), which can be prevented by blockade of iGluRs or KCC2 expression. In the course of TLE, hippocampal neurons can therefore embark on the strategy of cellular hypoactivity only if their Cl$^-$ equilibrium potential is low.

Acknowledgements

Supplementary material

The following supplementary material is available for this article:

Fig. S1 GlyRs a2A^{192L} and a2B^{192L} are high affinity receptors.
Supplemental information. Supplemental methods; results; reference; figure legend.

This material is available as part of the online article from:
http://www.blackwell-synergy.com/doi/abs/10.1111/j.1582–4934.2007.00357.x
(This link will take you to the article abstract).

Please note: Blackwell Publishing are not responsible for the content or functionality of any supplementary materials supplied by the authors. Any queries (other than missing material) should be directed to the corresponding author for the article.

References

1. **Stief F, Zuschratter W, Hartmann K, Schmitz D, Draguhn A.** Enhanced synaptic excitation-inhibition ratio in hippocampal interneurons of rats with temporal lobe epilepsy. *Eur J Neurosci*. 2007; 25: 519–28.

2. **Bouilleret V, Loup F, Kiener T, Marescaux C, Fritschy JM.** Early loss of interneurons and delayed subunit-specific changes in GABA(A)-receptor expression in a mouse model of mesial temporal lobe epilepsy. *Hippocampus*. 2000; 10: 305–24.

3. **Cossart R, Bernard C, Ben Ari Y.** Multiple facets of GABAergic neurons and synapses: multiple fates of GABA signalling in epilepsies. *Trends Neurosci*. 2005; 28: 108–15.

4. **Wang W, Xu TL.** Chloride homeostasis differentially affects GABA(A) receptor- and glycine receptor-mediated effects on spontaneous circuit activity in hippocampal cell culture. *Neurosci Lett*. 2006; 406: 11–6.

5. **Bedet C, Bruusgaard JC, Vergo S, Groth-Pedersen L, Eimer S, Triller A, Vannier C.** Regulation of gephyrin assembly and glycine receptor synaptic stability. *J Biol Chem*. 2006; 281: 30046–56.

6. **Meier J, Grantyn R.** A gephyrin-related mechanism restraining glycine receptor anchoring at GABAergic synapses. *J Neurosci*. 2004; 24: 1398–405.

7. **Zhang LH, Gong N, Fei D, Xu L, Xu TL.** Glycine uptake regulates hippocampal network activity *via* glycine receptor-mediated tonic inhibition. *Neuropsychopharmacology*. 2008; 33: 701–11.

8. **Song W, Chattipakorn SC, McMahon LL.** Glycine-gated chloride channels depress synaptic transmission in rat hippocampus. *J Neurophysiol*. 2006; 95: 2366–79.

9. **Mori M, Gähwiler BH, Gerber U.** Beta-Alanine and taurine as endogenous agonists at glycine receptors in rat hippocampus *in vitro*. *J Physiol*. 2002; 539: 191–200.

10. **Chattipakorn SC, McMahon LL.** Strychnine-sensitive glycine receptors depress hyperexcitability in rat dentate gyrus. *J Neurophysiol*. 2003; 89: 1339–42.

11. **Kirchner A, Breustedt J, Rosche B, Heinemann UF, Schmieden V.** Effects of taurine and glycine on epileptiform activity induced by removal of Mg^{2+} in combined rat entorhinal cortex-hippocampal slices. *Epilepsia*. 2003; 44: 1145–52.

12. **El Idrissi A, Messing J, Scalia J, Trenkner E.** Prevention of epileptic seizures by taurine. *Adv Exp Med Biol*. 2003; 526: 515–25.

13. **Miller PS, Harvey RJ, Smart TG.** Differential agonist sensitivity of glycine receptor alpha2 subunit splice variants. *Br J Pharmacol*. 2004; 143: 19–26.

14. **Nikolic Z, Laube B, Weber RG, Lichter P, Kioschis P, Poustka A, Mulhardt C, Becker CM**. The human glycine receptor subunit alpha3. Glra3 gene structure, chromosomal localization, and functional characterization of alternative transcripts. *J Biol Chem*. 1998; 273: 19708–14.

15. **Roux MJ, Supplisson S**. Neuronal and glial glycine transporters have different stoichiometries. *Neuron*. 2000; 25: 373–83.

16. **Wilson CL, Maidment NT, Shomer MH, Behnke EJ, Ackerson L, Fried I, Engel J Jr.** Comparison of seizure related amino acid release in human epileptic hippocampus versus a chronic, kainate rat model of hippocampal epilepsy. *Epilepsy Res*. 1996; 26: 245–54.

17. **Meier JC, Henneberger C, Melnick I, Racca C, Harvey RJ, Heinemann U, Schmieden V, Grantyn R.** RNA editing produces glycine receptor αβP185L resulting in high agonist potency. *Nat Neurosci*. 2005; 8: 736–44.

18. **Rivera C, Li H, Thomas-Crusells J, Lahtinen H, Viitanen T, Nanobashvili A, Kokaia Z, Airaksinen MS, Voipio J, Kaila K, Saarma M.** BDNF-induced TrkB activation down-regulates the K+-Cl- cotransporter KCC2 and impairs neuronal Cl-extrusion. *J Cell Biol*. 2002; 159: 747–52.

19. **Wake H, Watanabe M, Moorhouse AJ, Kanematsu T, Horibe S, Matsukawa N, Asai K, Ojika K, Hirata M, Nabekura J.** Early changes in KCC2 phosphorylation in response to neuronal stress result in functional downregulation. *J Neurosci*. 2007; 27: 1642–50.

20. **Palma E, Amici M, Sobrero F, Spinelli G, Di AS, Ragozzino D, Mascia A, Scoppetta C, Esposito V, Miledi R, Eusebi F.** Anomalous levels of Cl- transporters in the hippocampal subiculum from temporal lobe epilepsy patients make GABA excitatory. *Proc Natl Acad Sci USA*. 2006; 103: 8465–8.

21. **Davies KG, Hermann BP, Dohan FC Jr, Foley KT, Bush AJ, Wyler AR.** Relationship of hippocampal sclerosis to duration and age of onset of epilepsy, and childhood febrile seizures in temporal lobectomy patients. *Epilepsy Res*. 1996; 24: 119–26.

22. **Brewer GJ, Cotman CW.** Survival and growth of hippocampal neurons in defined medium at low density: advantages of a sandwich culture technique or low oxygen. *Brain Res*. 1989; 494: 65–74.

23. **Swartz ME, Eberhart J, Pasquale EB, Krull CE.** EphA4/ephrin-A5 interactions in muscle precursor cell migration in the avian forelimb. *Development*. 2001; 128: 4669–80.

24. **Lee H, Chen CX, Liu YJ, Aizenman E, Kandler K.** KCC2 expression in immature rat cortical neurons is sufficient to switch the polarity of GABA responses. *Eur J Neurosci*. 2005; 21: 2593–9.

25. **Golbs A, Heck N, Luhmann HJ.** A new technique for real-time analysis of caspase-3 dependent neuronal cell death. *J Neurosci Methods*. 2006; 161: 234–43.

26. **Pfeiffer F, Simler R, Grenningloh G, Betz H.** Monoclonal antibodies and peptide mapping reveal structural similarities between the subunits of the glycine receptor of rat spinal cord. *Proc Natl Acad Sci USA*. 1984; 81: 7224–7.

27. **Dumoulin A, Rostaing P, Bedet C, Levi S, Isambert MF, Henry JP, Triller A, Gasnier B.** Presence of the vesicular inhibitory amino acid transporter in GABAergic and glycinergic synaptic terminal boutons. *J Cell Sci*. 1999; 112: 811–23.

28. **Herzog E, Bellenchi GC, Gras C, Bernard V, Ravassard P, Bedet C, Gasnier B, Giros B, El Mestikawy S.** The existence of a second vesicular glutamate transporter specifies subpopulations of glutamatergic neurons. J Neurosci. 2001; 21: RC181.

29. **Williams JR, Sharp JW, Kumari VG, Wilson M, Payne JA.** The neuron-specific K-Cl cotransporter, KCC2. Antibody development and initial characterization of the protein. *J Biol Chem*. 1999; 274: 12656–64.

30. **Singh B, Henneberger C, Betances D, Arevalo MA, Rodriguez-Tebar A, Meier JC, Grantyn R.** Altered balance of glutamatergic/GABAergic synaptic input and associated changes in dendrite morphology after BDNF expression in BDNF-deficient hippocampal neurons. *J Neurosci*. 2006; 26: 7189–200.

31. **Salama-Cohen P, Arevalo MA, Meier J, Grantyn R, Rodriguez-Tebar A.** NGF controls dendrite development in hippocampal neurons by binding to p75NTR and modulating the cellular targets of notch. *Mol Biol Cell*. 2005; 16: 339–47.

32. **Ferrer I.** Neurons and their dendrites in frontotemporal dementia. *Dement Geriatr Cogn Disord*. 1999; 10: 55–60.

33. **Heinrich C, Nitta N, Flubacher A, Muller M, Fahrner A, Kirsch M, Freiman T, Suzuki F, Depaulis A, Frotscher M, Haas CA.** Reelin deficiency and displacement of mature neurons, but not neurogenesis, underlie the formation of granule cell dispersion in the epileptic hippocampus. *J Neurosci*. 2006; 26: 4701–13.

34. **Rivera C, Voipio J, Thomas-Crusells J, Li H, Emri Z, Sipila S, Payne JA, Minichiello L, Saarma M, Kaila K.** Mechanism of activity-dependent down-regulation of the neuron-specific K-Cl cotransporter KCC2. *J Neurosci*. 2004; 24: 4683–91.

35. **Levi S, Logan SM, Tovar KR, Craig AM.** Gephyrin is critical for glycine receptor clustering but not for the formation of functional GABAergic synapses in hippocampal neurons. *J Neurosci*. 2004; 24: 207–17.

36. **Liu G.** Local structural balance and functional interaction of excitatory and inhibitory synapses in hippocampal dendrites. *Nat Neurosci*. 2004; 7: 373–9.

37. **Ben-Ari Y.** Developing networks play a similar melody. *Trends Neurosci*. 2001; 24: 353–60.

38. **Turrigiano GG, Nelson SB.** Homeostatic plasticity in the developing nervous system. *Nat Rev Neurosci*. 2004; 5: 97–107.

39. **Lohmann C, Finski A, Bonhoeffer T.** Local calcium transients regulate the spontaneous motility of dendritic filopodia. *Nat Neurosci*. 2005; 8: 305–12.

40. **Talanian RV, Quinlan C, Trautz S, Hackett MC, Mankovich JA, Banach D, Ghayur T, Brady KD, Wong WW.** Substrate specifici-ties of caspase family proteases. *J Biol Chem*. 1997; 272: 9677–82.

41. **Chudotvorova I, Ivanov A, Rama S, Hubner CA, Pellegrino C, Ben Ari Y, Medina I.** Early expression of KCC2 in rat hippocampal cultures augments expression of functional GABA synapses. *J Physiol*. 2005; 566: 671–9.

42. **Loup F, Wieser HG, Yonekawa Y, Aguzzi A, Fritschy JM.** Selective alterations in GABAA receptor subtypes in human temporal lobe epilepsy. *J Neurosci*. 2000; 20: 5401–19.

43. **Kumar SS, Buckmaster PS.** Hyperexcitability, interneurons, and loss of GABAergic synapses in entorhinal cortex in a model of temporal lobe epilepsy. *J Neurosci*. 2006; 26: 4613–23.

44. **Martina M, Turcotte ME, Halman S, Tsai G, Tiberi M, Coyle JT, Bergeron R.** Reduced glycine transporter type 1 expression leads to major changes in glutamatergic neurotransmission of CA1 hippocampal neurones in mice. *J Physiol*. 2005; 563: 777–93.

45. **Supplisson S, Roux MJ.** Why glycine transporters have different stoichiometries. *FEBS Lett*. 2002; 529: 93–101.

46. **Behrens CJ, van den Boom LP, Heinemann U.** Effects of the GABA(A) receptor antagonists bicuculline and gabazine on stimulus-induced sharp wave-ripple complexes in adult rat hippocampus in vitro. *Eur J Neurosci*. 2007; 25: 2170–81.

47. **Harvey BD, Sloviter RS.** Hippocampal granule cell activity and c-Fos expression during spontaneous seizures in awake, chronically epileptic, pilocarpine-treated rats: implications for hippocampal epileptogenesis. *J Comp Neurol*. 2005; 488: 442–63.

48. **Sloviter RS, Zappone CA, Harvey BD, Frotscher M.** Kainic acid-induced recurrent mossy fiber innervation of dentate gyrus inhibitory interneurons: possible anatomical substrate of granule cell hyper-inhibition in chronically epileptic rats. *J Comp Neurol*. 2006; 494: 944–60.

49. **He XP, Kotloski R, Nef S, Luikart BW, Parada LF, McNamara JO.** Conditional deletion of TrkB but not BDNF prevents epileptogenesis in the kindling model. *Neuron*. 2004; 43: 31–42.

50. **Hartmann M, Heumann R, Lessmann V.** Synaptic secretion of BDNF after high-frequency stimulation of glutamatergic synapses. *EMBO J*. 2001; 20: 5887–97.

51. **Suzuki K, Sato M, Morishima Y, Nakanishi S.** Neuronal depolarization controls brain-derived neurotrophic factor-induced upregulation of NR2C NMDA receptor *via* calcineurin signaling. *J Neurosci*. 2005; 25: 9535–43.

52. **Zhang SJ, Steijaert MN, Lau D, Schutz G, ucinge-Vivier C, Descombes P, Bading H.** Decoding NMDA receptor signaling: identification of genomic programs specifying neuronal survival and death. *Neuron*. 2007; 53: 549–62.

53. **Burrone J, O'Byrne M, Murthy VN.** Multiple forms of synaptic plasticity triggered by selective suppression of activity in individual neurons. *Nature*. 2002; 420: 414–8.

54. **Tao HW, Poo MM.** Activity-dependent matching of excitatory and inhibitory inputs during refinement of visual receptive fields. *Neuron*. 2005; 45: 829–36.

55. **Trasande CA, Ramirez JM.** Activity deprivation leads to seizures in hippocampal slice cultures: is epilepsy the consequence of homeostatic plasticity? *J Clin Neurophysiol*. 2007; 24: 154–64.